Spring 5-2013

Analysis of brittle Paleogene structures in the Svea region, eastern Spitsbergen, Svalbard

Amanda LaFarge Goss
Bates College, agoss@bates.edu

Analysis of brittle Paleogene structures in the Svea region, eastern Spitsbergen, Svalbard

Bates College Geology Department Thesis

Presented to the Faculty of the Department of Geology, Bates College, in partial fulfillment of the requirements for the Degree of Bachelor of Science

by

Amanda LaFarge Goss

Lewiston, Maine
April 1st, 2013

Acknowledgments

Despite being a project of my own design, this thesis could not have been completed without the help of my Bates advisor Mitchell Scharman, who saw me through the mire of data analysis, interpretation and writing. For someone who may not have expected a senior thesis student to be foisted on him, he has done an incredible job encouraging me through the process, always available to talk about my questions and always prompt with constructive feedback. I hope, now that this project is concluded, that he can finally "enjoy the weekend".

I would also like to thank my advisor on Svalbard, Malte Jochmann, for sparking my initial interest in the geology of Svea and for his support through the course of the planning and fieldwork. The fieldwork would not have been possible without his involvement and enthusiasm for helicopters and steep slopes. The project itself was made possible through the logistical support of Store Norske and UNIS, so many thanks to all the folk in Svea, to Tomas Warnqvist and Bernt Holst for sharing data and information, and for the crew at UNIS logistics for outfitting the expedition. And of course, tusen takk to my incredible field partner Ane Svinth. I surely wouldn't have eaten so well without you!

To Dyk Eusden, Alvar Braathen and George Davis, thank you for sharing your wealth of knowledge about structural geology with me. Your input and ideas were essential when it came to formulating my interpretations. Thanks also to all my supporters here at Bates: the Bates Student Research Fund, and to Seri Lowell, Matt Duvall and William Ash for their respective editing, GIS and InDesign wizardry.

Lastly, a huge thank you to my family for instilling in me a love of the outdoors and geology.

And to the geo crew of '13, for being in this together.

Abstract

During the Paleogene rifting of Svalbard and Greenland along a dextral transform, deformation occurred in two stages. Initial transpression, which formed a fold-and-thrust belt in western Spitsbergen and a foreland basin in central Spitsbergen, was followed by transtensional rifting. Small-scale brittle structures are observed in the subhorizontal Paleogene strata on the foreland basin's eastern edge. This study analyzes the orientations and paleostress regimes of these structures in order to determine their tectonic origins. Orientation data from faults, joints, and slickenlines were collected within the Svea Nord mine and the surrounding area in order to resolve the paleostress regimes of these structures. An analysis of lineament orientations from aerial imagery was conducted to solidify these initial findings, based on the assumption that these linear erosional features are related to pre-existing bedrock fractures. Results show two populations of faults: NNW-SSE striking, west-dipping thrust faults and ENE-WSW striking normal faults. Joint orientation measurements reveal two dominant subvertical joint set orientations: ENE-WSW and NNW-SSE. The lineament data show a major NE-SW trend, and a minor NW-SE trend. Paleostress orientations of these structures suggest ENE-directed compression and NNW-SSE extension for the thrust faults and normal faults respectively. Given the age constraints on the faults and fractures, their orientations and paleostress determinations, they can be correlated with previously documented structures associated with fold-and-thrust belt deformation. That these small-scale extensional structures are likely related to the fold-and-thrust belt suggests that they formed in response to the larger dextral transpressive tectonic setting.

Contents

Table of Figures

Table of Tables

Introduction

The Svalbard Archipelago is located in the high arctic between 77° and 80° north latitude, north of Scandinavia. It sits on the northwest corner of the Eurasian plate, an uplifted part of the Barents Shelf (Jakobsson et al., 2012). It is bordered to the north by a sheared plate margin, the De Geer Transform or Hornsund Fault Zone, and to the north by a rifted margin, the Gakkel rift (Figure 1.1). Spitsbergen is the largest island in the archipelago, the other major islands being Nordaustlandet, Barentsøya and Edgeøya. 60% of Svalbard is glaciated (Ingólfsson, 2011), with major ice caps in north eastern Spitsbergen and Nordaustlandet (Figure 1.2).

Svalbard has been deformed by many tectonic events throughout its geologic history, most recently by its rifting from Greenland along a dextral transform during the Paleogene (66-23 Ma). Given the plate boundary geometry, an early transpressional phase occurred in the Paleocene and Eocene before transtensional rifting began in earnest in the Oligocene (e.g. Braathen & Bergh, 1995; Maher et al., 1995). Spitsbergen features two main structures resulting from this transpressional

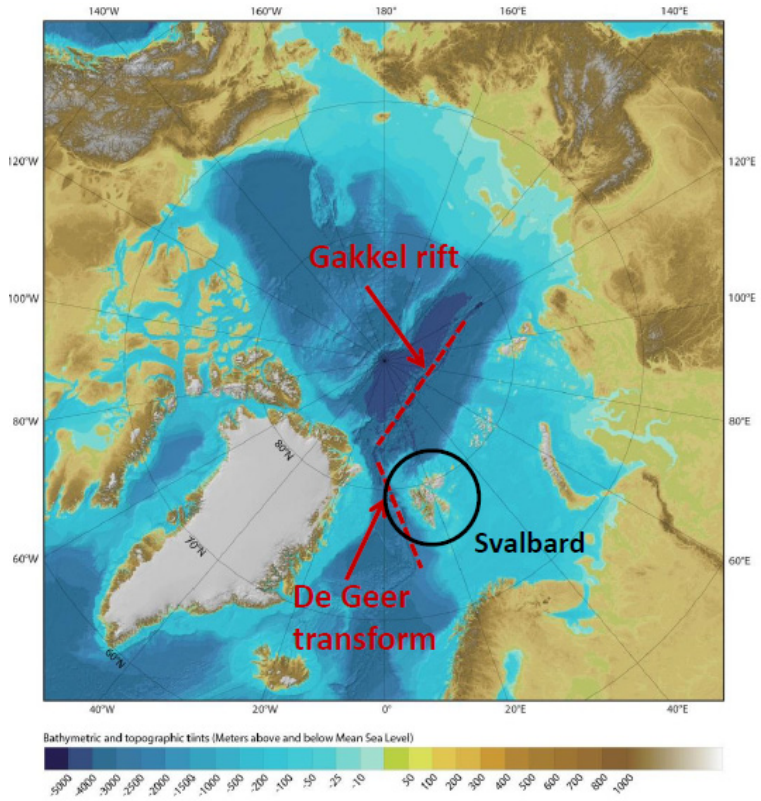

Figure 1.1 Bathymetric and topographic map of the Arctic Ocean showing the location of Svalbard at the edge of the Barents Shelf. The De Geer transform and the Arctic Ocean rift are also shown. (Jakobsson et al., 2012).

Figure 1.2 Bedrock geologic map of Svalbard showing main stratigraphic groups and fault zones (modified from Dallmann, 1999).

Figure 1.3 Bedrock geologic map of central Spitsbergen (Nordenskiøld Land) showing Central Tertiary Basin strata in yellow and the locations of coal mines. The mines currently operated by Store Norske are annotated. (Modified from Dallmann, 1999).

phase: a fold-and-thrust belt along the west coast and a large, associated foreland basin in the central part of the island. The Central Tertiary Basin, as it is known, contains Paleocene coal deposits that have been economically important to both the Norwegians and the Russians in the 20th century. This project focuses on the structural geology in the region of Spitsbergen's largest coal mine, Svea Nord, located at the head of Van Mijenfjorden in east-central Spitsbergen.

Svea is located on the eastern edge of the Central Tertiary Basin, where the stratigraphy is relatively flat-lying sandstone, shale, and coal deposits (Figure 1.3; Worsley, 1986). Although the region has not been strongly deformed by Paleogene tectonics, systematic small-scale normal faults and thrust faults are present. The Norwegian mining company Store Norske has considerable fault data from inside the mine, as offsets in the coal seam caused by the faults lead to delays in production. However, given the relatively small scale of these structures, no detailed structural studies on the faults or even on the structural geology of the region have been published to date. Therefore the faults' stress regimes and origins are currently unknown.

This study analyzes the brittle structures in the Svea region — normal and thrust faults, fractures in outcrops and aerial lineaments — in order to determine the direction of stresses on the rock at the time of deformation. Based on the orientations of these structures and their resolved paleostress regimes, the brittle deformation in the region can then be related to larger tectonic processes acting on Svalbard during the Paleogene.

Geologic Background

Tectonic History

Svalbard's geology spans the Precambrian through the Quaternary and the rock record is remarkably complete and relatively undeformed. It chronicles Svalbard's movement through time, plate configurations and climate zones. Since the Devonian, the archipelago has moved north from below the equator to its present position in the high arctic, as part of various tectonic plates. Svalbard has been transformed by many tectonic events: major deformation during the Middle Silurian Caledonide Orogeny, basin formation and subsequent deformation during the Devonian, rifting during the Carboniferous and transpression and extension during the Paleogene (Worsley, 1986; Dallmann, 1999; McCann and Dallmann, 1996; Worsley, 2008). Svalbard is presently in a period of tectonic quiescence, due to its relatively stable position on the edge of the Eurasian continental plate.

Paleogene Tectonics

Tectonic activity on Svalbard in the Paleogene was the result of the opening of the Norwegian-Greenland and Arctic basins (Worsley, 1986; Maher et al., 1986). An intercontinental transform margin linked these two spreading ridges. A combination of convergent and strike-slip tectonics resulted in both the dextral movement of Svalbard past Greenland and eastward-directed compression, which caused between 20 and 40 km of shortening in Western Spitsbergen (Dallmann, 1993; Braathen et al., 1999; Maher Jr. et al., 1986). This compression formed a fold-and-thrust belt along the west coast of Spitsbergen and a foreland basin in the east, where sediments were deposited (Figure 1.4a; Braathen et al., 1997; Leever et al, 2011).

The West Spitsbergen fold-and-thrust belt

The four regions of deformation associated with the fold-and-thrust belt consist of offshore hinterland extensional grabens (zone 1), a western basement-involved fold-thrust complex (zone 2), a central region of thin-skinned folded and thrusted strata above a major decollement (zone 3), and an eastern zone with a frontal duplex system

bounded to the east by steep reverse faults — the Billefjorden and Lomfjorden Fault Zones (zone 3) (Figure 1.4c; Haremo and Andresen, 1992; Bergh et al., 1997; Leever et al., 2011;). These two north-south trending fault zones have been periodically active in eastern Spitsbergen since the Caledonide Orogeny and were reactivated during the Paleogene activity (Worsley, 1986; McCann and Dallmann, 1996; Worsley, 2008). Most of the central and eastern deformation zones are covered by the relatively flat-lying strata of the Central Tertiary Basin.

Kinematic evolution of the fold-and-thrust belt

Extensive research, mainly by Braathen, Bergh and Maher, has focused on developing a model of the kinematic evolution of the West Spitsbergen fold-and-thrust belt, based on the orientation and relationship between structures along the length of the fold-and-thrust belt. They have developed a widely accepted five-stage kinematic model. Stage 1 is an initial northward-directed shortening in the Late Cretaceous – Early Paleocene. Stage 2 consists of major WSW-ENE shortening with in-sequence fold-thrust propagation in the foreland. Stage 3 is also ENE-directed, but features basement-involved uplift in the foreland and the reactivation of the Billefjorden and Lomfjorden fault zones, forming large-scale monoclines. Stage 4 features eastward out-of-sequence thrust propagation and associated strike-slip faulting, particularly in the basement-involved fold-thrust complex. Stage 5 consists of E-W extension, resulting in N-S striking normal faults in the hinterland and normal movement along the Billefjorden and Lomfjorden fault zones (Kleinspehn et al., 1989; Bergh et al., 1997; Braathen et al., 1997; Braathen et al., 1999; Leever et al., 2011).

Critical wedge model

To explain the 5-stage kinematic evolution of the fold-and-thrust belt, Braathen, Bergh and Maher have proposed a critical wedge model (Figure 1.4b; Braathen, Bergh and Maher Jr., 1999). Braathen and Bergh (1995) suggested that the stage 4-5 extension was due to the collapse of an overthickened fold-thrust complex or wedge. Braathen et al. (1999) state that a fold-thrust stack made up of crystalline basement and sedimentary cover rocks usually forms a wedge-shaped prism which then evolves toward a critical taper geometry. The wedge adjusts itself when the gravitational and compressive forces become greater than the basal friction force. Wedge geometry is controlled by the wedge growth rate, the strength of both the basal units and the detatchment surface, and the rate of erosion. Wedge theory premises that deformation will proceed in the wedge until a critical taper geometry is achieved. A weak basal layer will decrease the angle that the wedge can accommodate before it becomes unstable. An unstable wedge may respond with internal thickening, imbrication in the foreland and/or extension in the hinterland. A growing, east-tapered wedge model helps to explain the complexity of the fold-and-thrust belt,

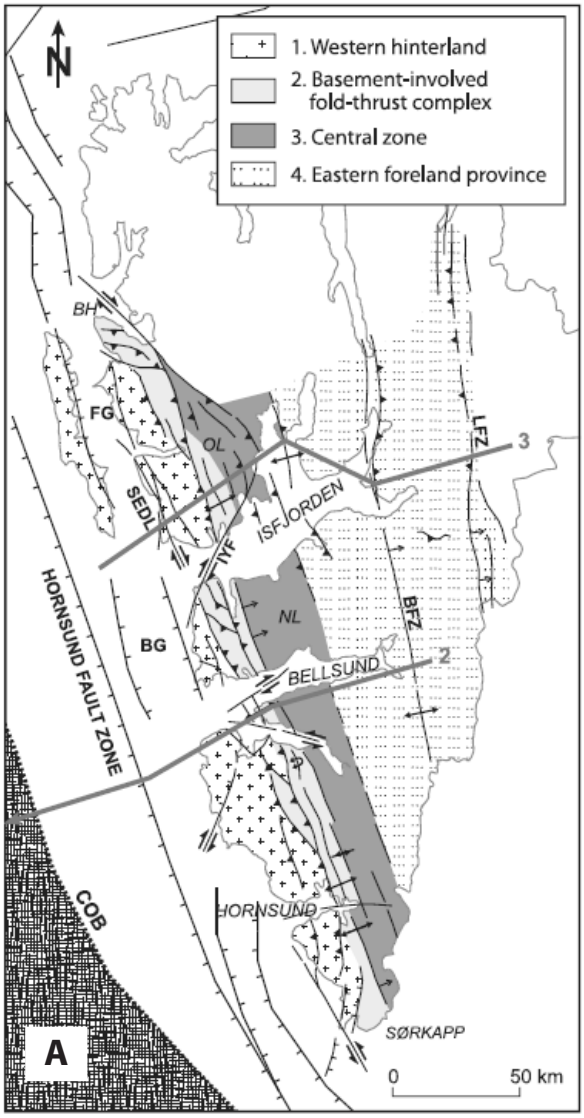

Figure 1.4 a) Structural geologic map showing the four major zones of the West Spitsbergen fold-and-thrust belt. Abbreviations: NL, Nordenskiöld Land; BFZ, Billefjorden Fault Zone; and LFZ, Lomfjorden Fault Zone (from Leever et al., 2011). b) Diagram and schematic cross-section describing critical wedge geometry and evolution. An overthickened wedge will adjust to a critical taper geometry through erosion and extension in the thickest part and thrust propagation towards the thinner wedge front. (from Braathen et al., 1999). c) Generalized cross-section through central Spitsbergen showing the four main deformation zones. Svea is located just west of the Billefjorden Fault Zone (BFZ). Note that the Paleogene cover rocks are not included in the cross-section (from Leever et al., 2011).

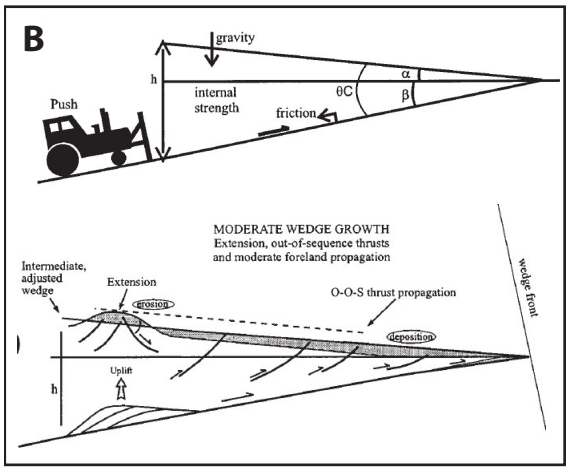

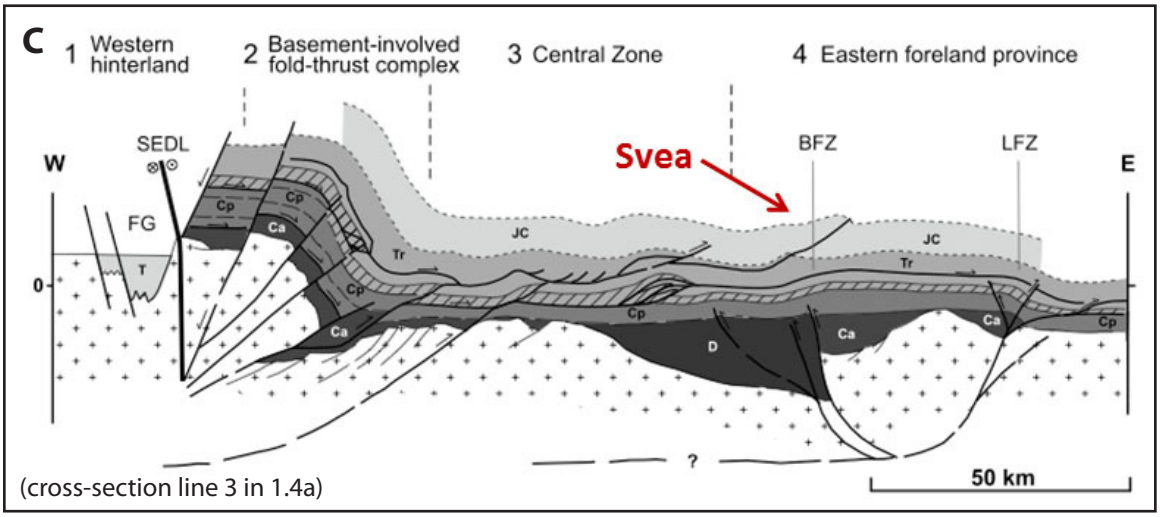

including the timing and relationship of fold-thrust structures (Braathen et al., 1999). One possibility for the origins of the normal faults in the Svea area is that they are related to the collapse of this overthickened crustal wedge.

Regional Stratigraphy

The foreland basin that formed in conjunction with the West Spitsbergen fold-and-thrust belt during the transpressional tectonic regime of the Paleogene is called the Central Tertiary Basin and covers much of south-central Spitsbergen (Figures 1.2 and 1.3). As the crustal wedge in the west thickened, the surrounding terrain subsided, resulting in both hinterland and foreland basins. Sediments eroded off the newly uplifted fold-and-thrust belt were deposited in the foreland basin. The stratigraphy of the Central Tertiary Basin evidences its changing morphology and sedimentation rates throughout the Paleogene.

Carolinefjellet Formation

The Carolinefjellet Formation, of Early Cretaceous age, is not part of the Central Tertiary Basin fill but lies directly beneath the Paleogene strata throughout Spitsbergen. It consists of interbedded sandstones and shales and features hummocky cross-stratification, evidence of large storm events (Dallmann, 1999). The Carolinefjellet Formation is exposed in the lower slopes of the mountainsides of the Svea region.

Firkanten Formation

The lowermost Paleocene formation is the Firkanten Formation, and is critical to this study as it contains the most important coal deposits on Svalbard. It has a basal low-angle unconformity with the Carolinefjellet Formation and consists of two formations: the lower coal-bearing Todalen Member and the upper sandstone-dominated Endalen Member. The Todalen Member contains three to five shale-siltstone-sandstone-coal successions, indicative of a naturally prograding delta system. The Endalen Member contains four to five well bioturbated and cross-stratified cliff-forming sandstone units, which are indicative of a high-energy near shore environment. The Firkanten Formation represents a general transgression from coastal plain to shallow marine environment that is pre-fold-and-thrust belt (Dallmann, 1999).

Basilika Formation

Above the Firkanten Formation is the Basilika Formation, also of Paleocene age, which consists entirely of soft shales. It represents a rapid transgression as a result of subsidence of the foreland basin, signaling the onset of fold-and-thrust belt activity (Dallmann, 1999). The Basilika Formation is relatively thin in the Svea region and is so erodible that no outcrops are seen.

Grumantbyen Formation

The Grumantbyen Formation is the uppermost Paleocene strata and consists of black to green heavily-bioturbated sandstones: shelf deposits. The presence of glauconite indicates low sedimentation rates and the formation shows a general regression. This suggests to a pause or decrease in the rate of uplift of the fold-and-thrust belt (Dallmann, 1999). The Grumantbyen Formation is the uppermost stratigraphic unit which outcrops in the mountains of the study area.

Mining on Svalbard

Svalbard has a history of coal mining, starting in the early 20th century with the opening of the first mine in Longyearbyen. Because the thickest coal seams are in the Todalen Member in the lowermost layer of the Paleogene stratigraphy, coal has been mined where it outcrops at the edges of the Central Tertiary Basin (Figure 1.3). Today, Todalen coal is mined by the Norwegian mining company Store Norske in Longyearbyen and Svea and by the Russians in Barentsburg. The coal mined outside of Longyearbyen at Mine 7 is mainly used to power the town's electrical plant while all of the coal from the Svea Nord mine in Svea is exported to Germany and other European countries (Store Norske Spitsbergen Kulkompani, AS, 2012).

Svea Nord is by far the largest coal mine on Svalbard. It extends over 18 km below the mountains and glaciers north of Braganzavågen, at the head of Van Mijenfjorden. The Svea seam is consistently thick, up to 5 m thick in places, and consists of high-volatile bituminous coal (Jochmann, pers. comm., 2/29/12). Store Norske uses a technique called long-wall mining to extract the coal. The coal is cut out in strips 250 m wide, starting at the back of the mine and moving toward the entrance. The roof of the coal seam and the rocks above it then collapse into the void formed by the extracted coal.

Even small faults are important to Store Norske because they cause serious delays in mining production. A small, meter-scale offset in the coal seam caused by a fault can halt the long-wall machine, as it cannot efficiently cut through the shale that lies above and below the coal. Hence, Store Norske has been careful to map all faults they

have come across during the excavation of the mine's transport tunnel network, in the hopes of being able to predict where these faults might occur in the strips slated for mining. In addition to using fault data to determine paleostress regimes, this study looks at fault orientation data to find the approximate location of faults in the strip to be mined this year.

Study Area

The study area is an approximately a 36 km^2 mountainous area surrounding the Svea Nord mine entrance (Figure 2.1). It is bordered by Höganäsbreen to the south, Feiselen to the west, Stempelen to the north, and Kolhamaren to the east. The elevation varies from about 350 m.a.s.l. at the mine entrance to 900 m.a.s.l. at the summit of the Gruvefonna ice cap (Norwegian Polar Institute, 2012). A significant portion of the study area is covered by glaciers and the remaining unglaciated areas are quite steep and often covered with either frost-shattered loose rock or permanent snow fields.

The stratigraphy in the study area is relatively flat-lying, with dips less than 15° WSW (Salvigsen et al., 1989). The Svea seam itself dips about 5° SW (Jochmann, pers. comm., 7/2012). The lowermost slopes of the mountains in the study area are made up of Carolinefjellet Formation. Their mid-upper slopes consist of the cliff-forming Firkanten Formation, erodible Basilika Formation and cliff-forming Grumantbyen Formation. Some mountains have plateau summits formed by the top of the sturdy Grumantbyen formation, while others have rounded tops of the erodible Frysjaodden shales. Outcrops are generally confined to the more resistant cliff-forming units such as the Endalen Member and Grumantbyen Formation. The faults which are clearly visible in the mine are difficult to observe on the landscape except where they cut through and offset these sandstone units.

The brittle structures in the study area — normal and thrust faults, joints and lineaments — are key to understanding the deformational history of the rocks since they were deposited in Paleocene. The stress regimes defined by the orientations of these structures can help reveal their tectonic origins in the context of the overall transpressive system acting on Svalbard during the Paleocene-Eocene.

Methods

Overview

Orientation data from brittle structures were collected in a 36 km^2 region above the Svea Nord mine, in order to determine regional paleostress. The following methods for paleostress reconstruction rely on the assumption that all brittle structures in the area formed under the same stress regime sometime after the Paleocene deposition of the sediments. In the field, the orientation and sense of movement was measured for faults exposed in surficial locations and for faults exposed in the mine. Orientations of systematic joints in outcrops and slickenlines on exposed fault planes were also measured. The joint data were then analyzed using Stereonet 8 (Allmendinger, 2012a) and the slickenline data were analyzed with FaultKin 5 (Allmendinger, 2012b) to get a sense of the region's paleostress regime at the time of structure formation. An analysis of linear features from aerial imagery and digital elevation models was conducted using ArcGIS to complement the field analysis and to reinforce the paleostress determinations. In addition, both existing structural data from Store Norske and present day earthquake data were compared to the results to better constrain the paleostress and tectonic regime.

Fieldwork

Faults and fractures were mapped in the field area in July 2012. Primarily, offsets in the stratigraphy and slope geomorphology were used to locate the surficial faults. As fault rocks are weaker and tend to weather more quickly, gullies and more eroded areas can be clues to fault locations. The approximate orientation and throw of the faults were determined by sighting across valleys from positions in-line with the apparent strike of the faults.

Faults were also mapped within the southeastern part of the Svea Nord mine. Fault mapping was done in the H1, H2, H-8, and HT-3 sections of the mine (Figure 3.5). Fault orientations were measured directly on the fault planes where they were exposed, by sighting across the tunnels, or along ceiling exposures. The orientations of prominent slickenlines both on the fault planes and within a 2 m radius of the faults were recorded. Fault throw was measured using a meter stick or a laser distance-measuring device.

Joint orientations were measured in accessible outcrops in four localities (Figure 2.1). Joints were typically measured in transects along the outcrop face for 20-50 m. Site 1, on the west side of Boret, was located within the Firkanten Formation sandstone, as

was site 2 on the south side of Boret and site 3 at Stempelen. Site 4 was located on the west side of Boret within the younger Grumantbyen Formation sandstone.

Paleostress Analysis of Brittle Structures

In regions of relatively undeformed sedimentary strata, paleostress orientations can be determined by slickenlines on fault planes, which record fault slip, and small-scale brittle structures, such as joints (Dunne and Hancock, 1994; Angelier, 1994). Though slickenlines are more reliable paleostress indicators, the lack of exposure of fault planes in the above-ground field area confined measurements of slickenlines to fault planes exposed in the mine. Joint orientations were measured in accessible outcrops in four localities in the field area, to better constrain paleostress orientations (Figure 2.1).

Conjugate joint set analysis

Though not as reliable as slickenlines, joints can also be used to reconstruct paleostress Systematic joints are caused by deep-seated stress fields and therefore can be used as paleostress indicators (Fossen, 2010; Davis, 2011). Where no cross-cutting

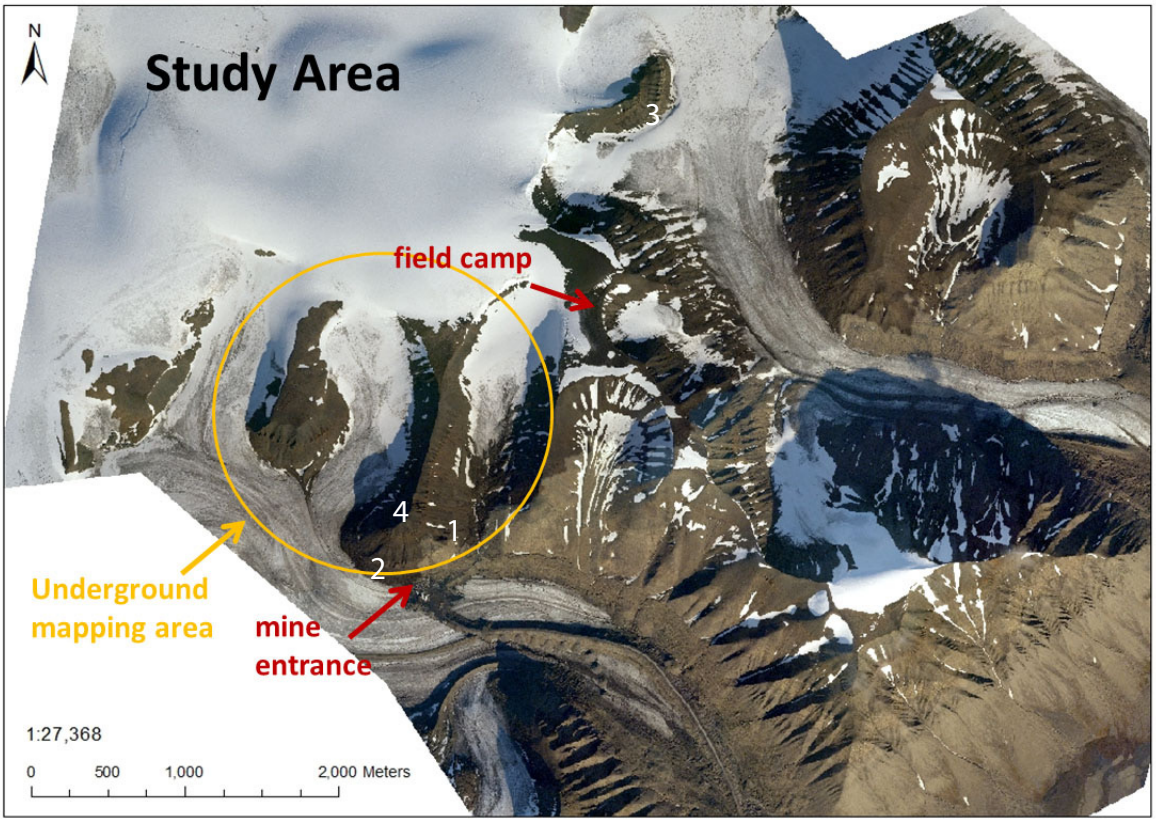

Figure 2.1 Orthoimage of the above-ground field area, showing the approximate location of the underground mapping area. Note the steep topography and high percentage of glacial and snow cover. The locations of joint data collection, sites 1-4, are also shown.

relationships are observed, joint sets are assumed to be conjugate, forming at the same time under the same stress regime. Conjugate joint sets are the most useful paleostress indicators, as both the type of joints and the orientations of the principle stress axes can be determined (Dunne and Hancock, 1994). In a simple conjugate joint system, σ_2 is located at the intersection of the two joints, σ_1 bisects the angle between them, and σ_3 is oriented perpendicular to both σ_1 and σ_2 (Figure 2.2; Bons et al., 2012). Based on these assumptions, the joint measurements were plotted as planes, poles-to-planes and rose diagrams using Stereonet 8 (Allmendinger, 2012a), to determine the primary stress axes σ_1, σ_2, and σ_3.

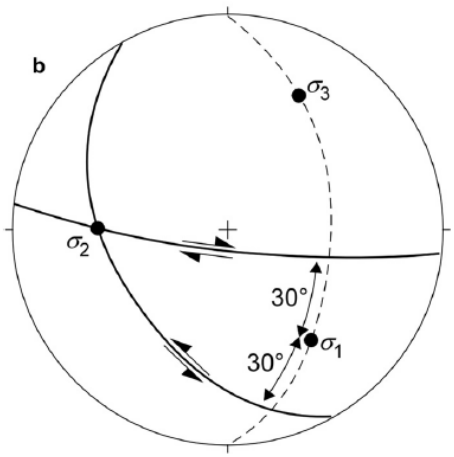

Figure 2.2 Stereonet plot of a conjugate joint set to determine principle stress axes. Note that σ_1 bisects the acute angle between the two joints, σ_2 is located at the intersection of the two joints, and σ_3 is perpendicular to both. Figure modified from Bons et al., 2012.

For each site's data, the average pole for each joint set was calculated by selecting the joints with similar orientations and using the Bingham axial distribution tool, which gives the cylindrical best fit for a set of poles. Planes were then calculated from these poles using the "planes from poles" tool. The acute angle between the two average joint set planes was then calculated.

Fault slip analysis

Orientations of slickenlines were measured on exposed fault planes inside the Svea Nord mine. Where fault planes were not exposed, a number of measurements were taken of slickenlines on minor shear planes nearby (less than 2 m). Although not a direct measurement of fault slip, the slickenlines from these planes can give some idea about the general direction of movement proximal to the fault. Because the coal was deformed in areas proximal to the faults, resulting in slickensides of varying orientations, these measurements were averaged and correlated with the nearest fault.

A number of assumptions must be made when using slickenlines for paleostress determination. The critical assumption is that slickenlines represent the direction of slip on the fault plane and are therefore are parallel to the direction of maximum shear stress. The second assumption is that a population of sampled faults have slipped in response to the same stress regime or homogeneous stress field. Other assumptions include that movement on one fault has no influence on the movement of other faults and that there has been no reorientation by later deformation (Angelier, 1994). Given the geologic context of this study and these assumptions, slickenline orientations

from faults within the mine and a fault at the surface were analyzed for fault slip paleostress solutions using the program FaultKin 5 (Allmendinger, 2012b). The linked Bingham analysis tool was run on data from 7 fault planes with slickenlines in order to determine the regions of compressive and tensile stress and thereby the paleostress orientation.

Lineament analysis

A three-part lineament analysis was conducted, based on methods by Mabee et al. (1994), to reinforce the paleostress determined from the conjugate joint set and fault slip analyses. It consisted of 1) lineament mapping, 2) reproducibility tests and 3) domain overlap analysis (e.g. Mabee et al., 1994; Castro, 2010; Kindley, 2011).

Lineament mapping involved tracing all linear features in the study area, excluding glacial and periglacial features and lineaments clearly related to the flat-lying stratigraphy, in ArcGIS on three images: an orthophoto acquired from Store Norske, photoshop-merged aerial photographs from the Norwegian Polar Institute (NPI), and a 20 m-resolution digital elevation model (DEM) acquired from Markus Eckerstorfer at UNIS. Shapefiles were created for the lineaments observed on each image. In order to determine the length and orientation of these lineaments, coordinate geometry (COGO) fields were applied to the attribute tables of each shapefile. Running the COGO tool produced the azimuth and length of each lineament.

Reproducibility tests were then designed to remove all irrelevant lineaments from the data set. According to Mabee et al. (1994), the three images should be superimposed at the same scale and coincident lineaments with azimuths within 5° and a separation distance of 1-2 mm at scale of observation should be selected and all other non-coincident lineaments should be discarded. Due to problems with the initial georeferencing of the NPI aerial photographs, the NPI lineament shapefile was rasterized and then re-georeferenced in order to make the comparison between images possible. The corrected NPI lineaments were then visually compared to the orthophoto and DEM lineaments at a 1:2000 scale. All lineaments that did not reproduce over at least two images were discarded from the analysis.

The domain overlap analysis compared the dominant joint orientations at each joint mapping locality to nearby lineaments. The field area was first divided into six sub-areas, each encompassing mountain or an area of concentrated lineaments. Rose plots were constructed at 5° intervals for each lineament sub-area to determine the dominant orientations for each region. The lineament orientations were then compared to the dominant joint set orientation data where available. As joints were only measured at four sites in the western part of the study area, lineaments in the eastern part of the study area had no direct joint comparison.

Results

Joint analysis

Field observations

In the study area, the sedimentary stratigraphy was subhorizontal, dipping less than 15° W (Figure 3.1a). Systematic, subvertical joints were observed in sandstone outcrops at all four mapping sites in the field area (Figure 3.2a). At site 4 in the Grumantbyen Formation, both cross-cutting relationships and curved joints were observed (Figure 3.2). Joints trending N-S were truncated at joints trending E-W. However, similar cross-cutting relationships were not observed at the other mapping sites in the Firkanten Formation, indicating that they are perhaps formation-specific features. Therefore, these joint relationships cannot be applied to the entire field area.

Conjugate joint set orientations and paleostress

Given the lack of clear cross-cutting relationships at the majority of the mapping sites, all joints were assumed to be conjugate. The 121 joint orientation measurements from all four outcrop areas show two dominant sub-vertical joint orientations: a major ENE-WSW trend and a minor NNW-SSE trend (Figure 3.1b). The calculated average joint set orientations for each site are presented in Table 1. Joint set 1 is generally

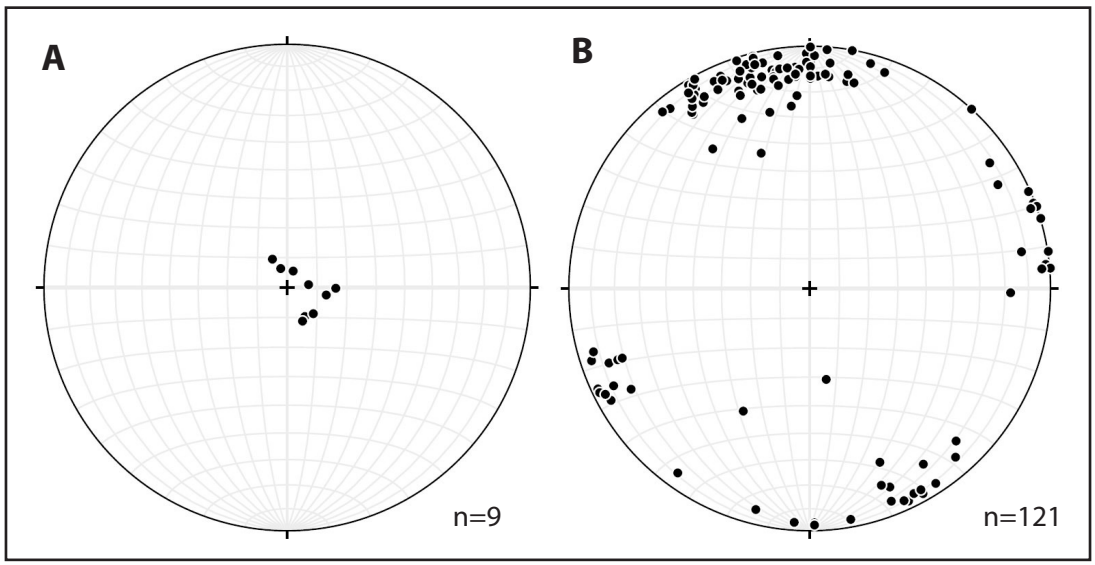

Figure 3.1 Equal angle lower hemisphere stereonet plots of poles to planes of: a) bedding measured at each fracture mapping site. The average orientation of bedding is 189, 6° W. b) all joints measured at the 4 outcrops in the study area. Note the two dominant concentrations of poles, corresponding to two dominant sets of sub-vertical joints (ENE-WSW and NNW-SSE striking).

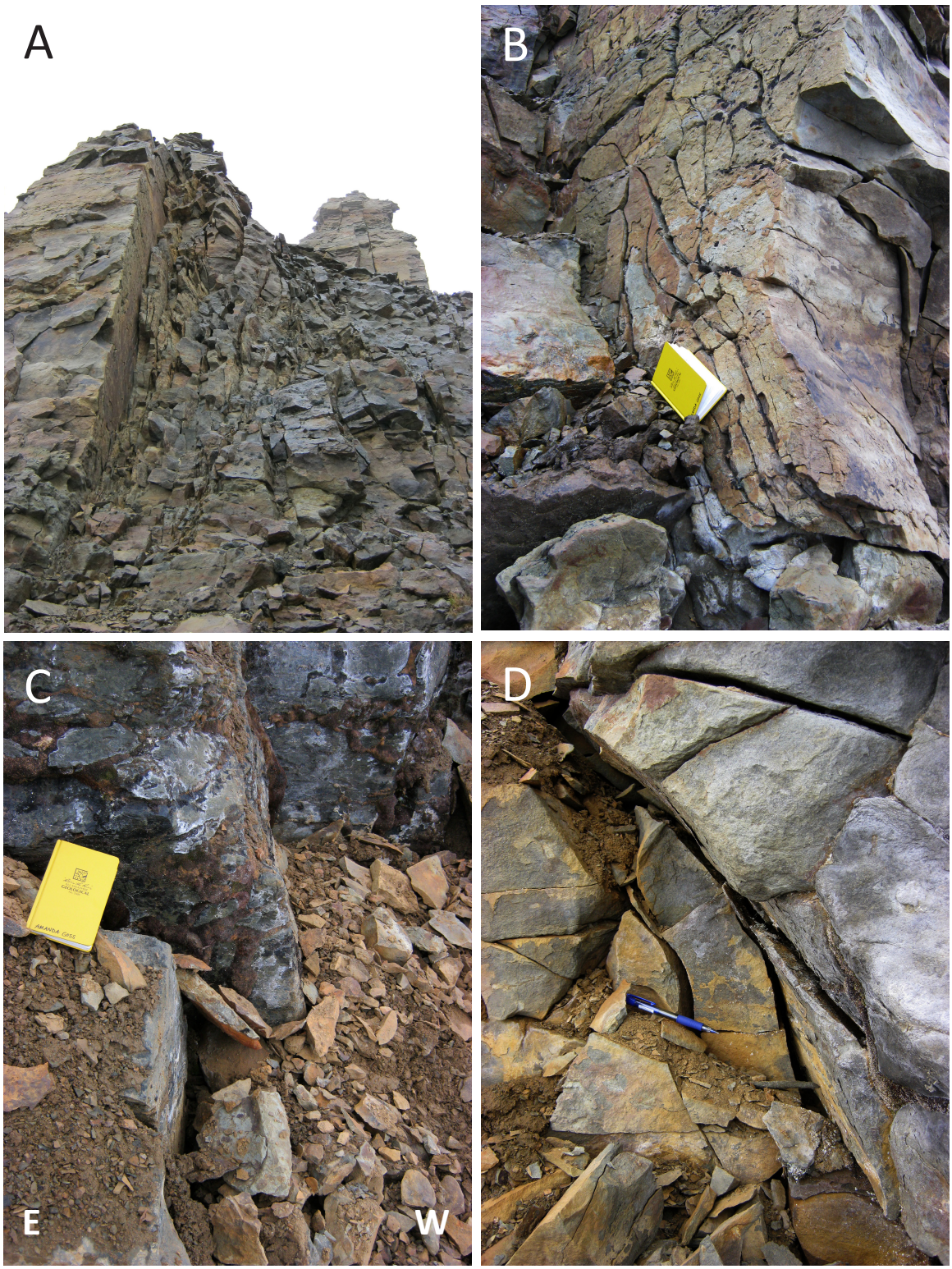

Figure 3.2 Photographs of joint characteristics. a) Example of subvertical, throughgoing joints at site 1. b) Predominant vertical joint face exposed at site 1. c) Cross-cutting relationships between the two dominant joint sets observed at site 4. The N-S trending joints truncate at the E-W trending joints. d) Curved joints observed at site 4.

ENE-WSW striking and subvertical, dipping between 82° and 89°N at the four sites. Joint set 2 is generally NNW-SSE striking and subvertical, with dips ranging from 79°E to 87°W. The acute angles between the two average joint sets at all sites are relatively large, ranging from 73° to 82° (Table 3.1).

The principal stress axes σ_1, σ_2 and σ_3 (σ_1 is defined here as the greatest compressive stress) resolved through the analysis of the conjugate joint sets at each site are presented in Stereonet diagrams in Figure 3.3. Given the sub-vertical orientation of the average joint sets, both the maximum principal stress (σ_1) and the minimum principal stress (σ_3) are oriented sub-horizontally for all joint sets. Since σ_2 is defined as the intersection of the two joints in a conjugate joint system (Bons et al., 2012), it is oriented subvertically for all sites. Though the orientations of the average joint sets at each mapping site are fairly similar (Table 3.1), the sites show differing orientations of maximum principal stress because of the magnitude of the acute angles. Sites 1 and 3 have the greatest principal stress in a NW-SE direction, while sites 2 and 4 have the greatest principal stress in a NNE-SSW direction (Figure 3.3).

Site	**Joint set 1** (strike, dip, dip direction)			**Joint set 2** (strike, dip, dip direction)			**Acute angle**
1	78	82	N	155	87	W	77
2	69	84	N	167	89	W	82
3	84	89	N	156	79	E	73
4	53	84	N	157	90	W	77

Table 3.1 The average joint set orientations calculated from the joint data from mapping sites 1-4 in the Svea region. Joint set 1 trends ENE-WSW and joint set 2 trends NNW-SSE. All values are in degrees from N. The acute angle is the smaller angle between the two average joint set planes at each site.

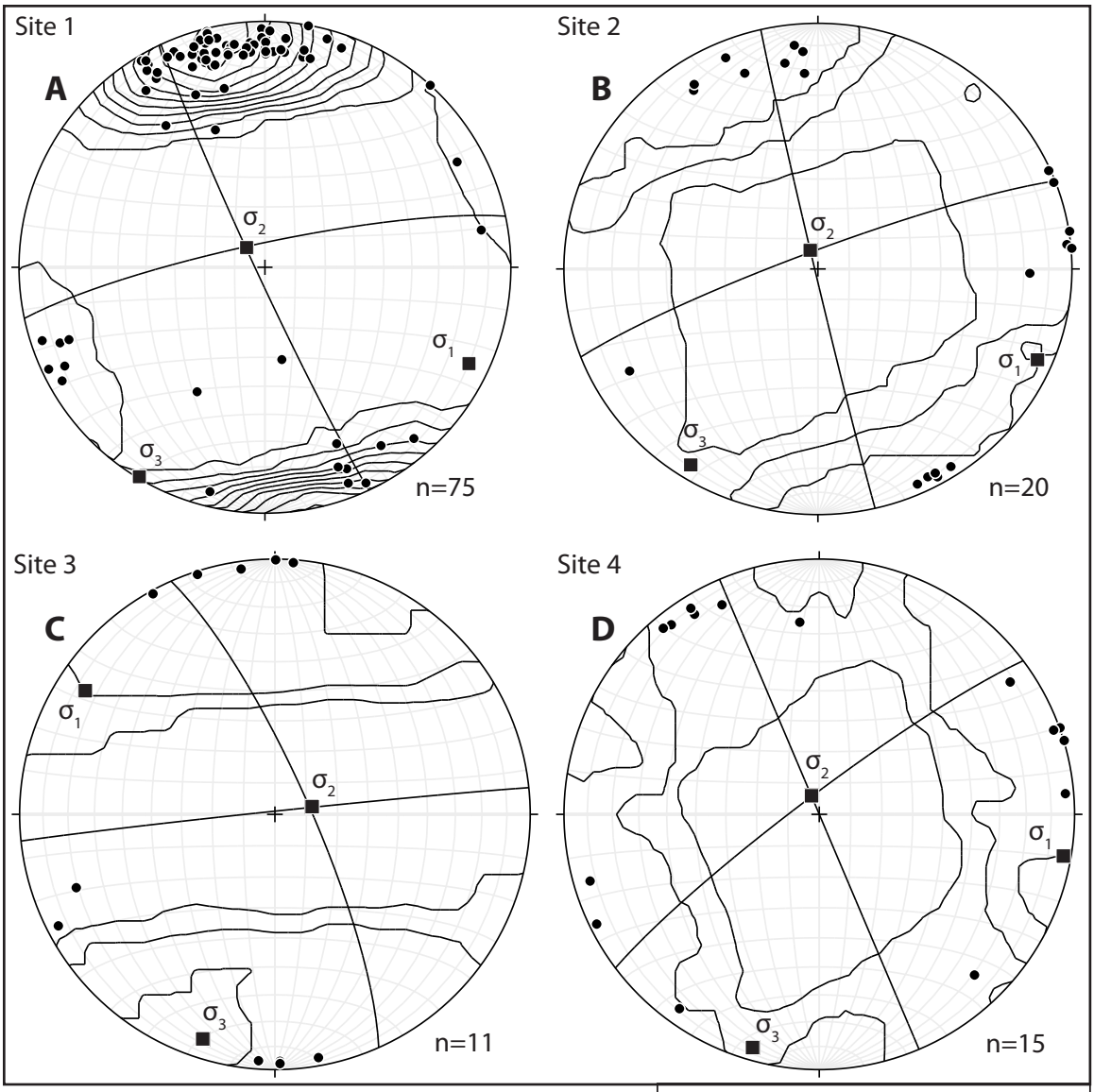

Figure 3.3 Stereonet lower hemisphere equal area plots of poles to joint planes measured at sites 1-4 and contoured using the Kamb method. Also included are the planes of the two conjugate joint sets, and the principal stress axes resolved from them. a) At site 1, a dominant E-W joint set and a less dominant NNW-SSE set are seen b) At site 2, a dominant ENE-WSW joint set and a less dominant N-S set are seen, but c) At site 3, a dominant E-W joint set and a less dominant NNW-SSE set are seen. d) At site 4, a dominant NE-SW joint set and a less dominant NNW-SSE set are seen. Given the quantity of data at site 1, its paleostress regime of σ1 oriented NW-SE is applied to sites 2 and 4, despite the discrepancy in the orientation of the acute angle at these sites.

Fault analysis

Fault orientations

Three normal faults in observed in the east slope of Boret near site 1. The largest fault was located in a gully in the mountainside and showed a minimum of four meters of offset in the stratigraphy (Figure 3.4a). The Boret faults strike approximately E-W and have apparent dips ranging from 55-65° (Table 3.2). A low-angle normal fault, striking NW-SE and dipping 32° SW, was exposed at site 3 (Figure 3.4b, Table 3.2). A total of 15 normal faults or fault branches were mapped within the mine, striking NE-ENE and dipping either NW or SE (Table 3.2). Fault throw is given for faults with measurable offset bedding. The locations of all faults can be seen in Figure 3.5. Small-scale SW dipping thrust faults, previously mapped by Store Norske, strike approximately perpendicular to the normal faults. Though none of these thrust faults were mapped during this study, due to their inaccessibility, they are important to consider when thinking about the paleostress of the fault system.

Because of their orientations, faults 5, 6, 7 and 8 can be interpreted as part of the same NE-SW-trending and NW-dipping fault system, with a total cumulative throw of about 4 m. Minor faults with less than 20 cm of throw were associated with this fault system, as they split and merge along the fault zone. Some shearing and deformation of the coal near the faults was observed, resulting in many slickenlined surfaces with varying orientations (Figure 3.4c).

Fault throw and displacement

The amount of throw, defined as the vertical distance by which the fault offsets the stratigraphy, is shown in Table 3.2 for all faults mapped in the mine. The strikes of faults 1 through 5 are approximate, as their orientations were previously mapped by Store Norske and obtained from their map. The letters in the fault ID denote multiple branches of the same fault system in a given location. Additionally, faults 5 and 6 can be correlated and are part of the same fault system. The amount of throw on each fault branch is relatively small, ranging from 0.32 m to 4 m. The cumulative throw of all fault branches at fault location 5 is 2.75 m while the cumulative throw of all fault branches at location 6 is 4.22 m. The actual displacement along the fault planes, calculated for faults with both dip and throw data, is also shown in Table 3.2.The dips of the fault 5 branches are approximate because the fault planes were not exposed. Displacement along all fault branches is slightly greater than the fault throw, ranging from 0.39 m to 2.23 m.

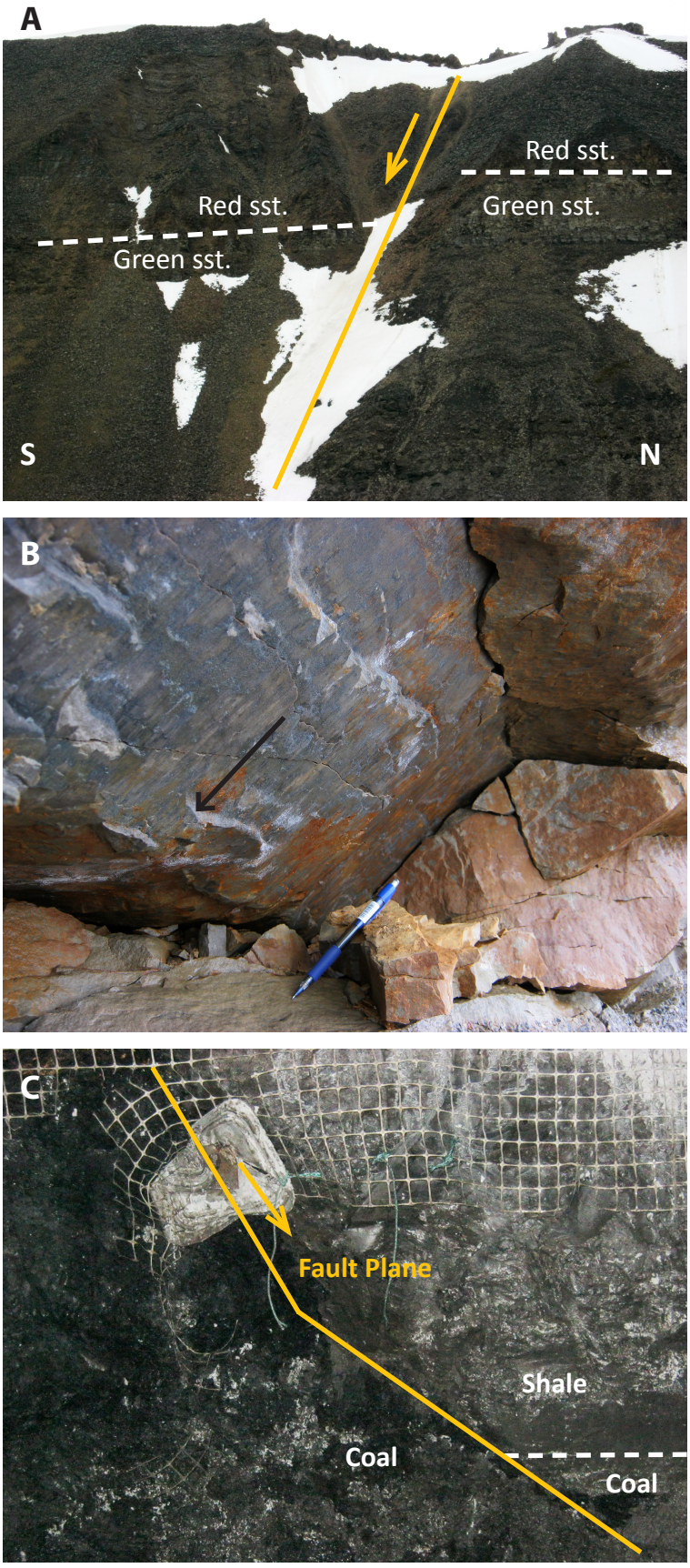

Figure 3.4 Annotated photographs of faults observed in the field area. a) Normal fault (fault 10) exposed in the E side of Boret, in the Grumantbyen Formation, near site 1. The offset in the stratigraphy is clear by the change in height of the boundary between the red and green sandstone beds. The fault and its motion are annotated in yellow. b) Fault plane (fault 9) exposed in the outcrop (Firkanten Formation) at site 3. Slickenlines in the hanging wall show normal movement (represented by arrow). The orientation of this fault was 166°, 32° W. c) Normal fault segment (8b) exposed in the Svea Nord mine. The top of the coal seam (white dashed line) is offset 1.8m. The fault and its movement are annotated in yellow. The coal in the footwall has been sheared and multiple shiny slickenlined surfaces are exposed.

Location	Fault ID	Strike (°)	Dip (°)	Dip direction	Slip	Throw (m)	Displacement (m)
H1	1	≈ 67	70	SE	normal	1.50	1.60
	2	≈ 67	70	SE	normal	2.00	2.13
	3	≈ 67	65	SE	normal	4.00	4.41
	4	≈ 67	70-80	SE	normal	1.00	1.04
H2-26	5a	≈ 52	≈ 50	NW	normal	0.4	0.52
	5b	≈ 52	≈ 60	NW	normal	1.4	1.62
	5c	≈ 52	≈ 60	NW	normal	0.6	0.69
	5d	≈ 52	≈ 65	NW	normal	0.35	0.39
H8-2	6a	83	73	NW	normal	4	4.18
	6b	65	37	NW	normal	0.2	0.33
	6b	60	50	NW	normal	0.2	0.26
HT-3 B	7	58	61	NW	normal		
HT-3-4 A	8a	67		NW	normal	2.1	2.23
	8b	61	64	NW	normal		
	8b	68	68	NW	normal	1.8	1.99
	8b	69	63	NW	normal		
	8c	53	87	NW	normal		
	8c	72		NW	normal	0.32	0.40
	8d	77		NW	normal		
	8d	60		NW	normal		
	8d	74	47	NW	normal		
	8d	51	59	NW	normal		
Site 3	9	166	32	NW	normal		
Site 1	10	≈ 90	65	S	normal	4	4.41
	11	≈ 90	55	S	normal	0.5	0.61
	12	≈ 90	57	S	normal	0.5	0.60

Table 3.2 Orientation and throw data for all faults mapped in the study area both inside and outside the mine. All faults show normal slip. Faults 1-8 were located within the mine, while faults 9-12 were mapped at the surface. The approximate strike of faults 1-5 is obtained from an unpublished Store Norske mine map. The approximate dips of the fault 5 branches were estimated from a field sketch, as no fault planes were exposed. The strikes of faults 10, 11 and 12 were estimated based on their exposure in the Boret mountainside. The letters after the fault number ID indicate different branches of the same fault system in a given location. Displacement calculated for faults with known dip and throw is also shown. The locations of the faults can be seen in Figure 7.

Fault slip analysis

The results of the fault slip analysis of fault planes with clear slickenlines show similar directions of fault slip for faults in the mine and a very different direction of slip for fault 9 at mapping site 3 (Figure 3.6a). The mine faults have a general NNW slip direction, while fault 9 has an ESE slip direction. As there is no way to determine whether these faults formed under different stress regimes, they are assumed to have formed under the same stress regime. The FaultKin stress tensor diagram (Figure 3.6b) shows the resolved compressional and tensional regions and the principal stress axes. The unshaded region represents the region of compression, while the shaded regions represent regions of tension. It follows that σ_1 is oriented vertically, which is typical of normal faults, that σ_2 is oriented parallel to the majority of the fault planes, and that σ_3 is oriented perpendicular to both, in a NNW-SSE direction.

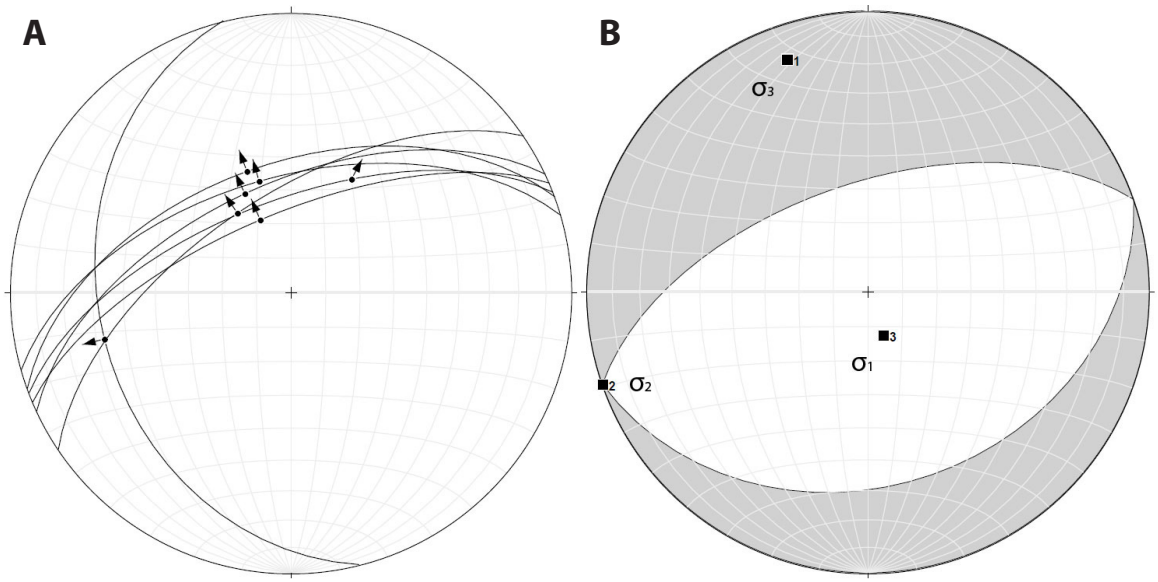

Figure 3.6 (a) Stereonet diagram showing fault planes and direction of slip as indicated by slickenlines. (b) Stress tensor diagram showing regions of compressive stress (unshaded) and regions of tensional stress (shaded). The principal stress axes are also shown.

Lineament analysis

A total of 3,180 lineaments were traced on the three images: 1,935 on the orthophoto, 1,132 on the merged aerial photos, and 113 on the hillshade image of the 20x20m DEM (Figures 3.7, 3.8 and 3.9). Of these lineaments, 883 were reproducible across at least two of the three images (Figure 3.10). The orientations of these reproducible lineaments from subdivided areas of the Svea region are shown in rose plots in Figure 3.10. Joint orientation data is also shown where available as a comparison.

Though the lineament orientations are variable in each subarea, most areas show a general NE trend (Figure 3.10). The lineament orientations do not correlate perfectly with the joint orientations, but this is to be expected given the wide spatial distribution of lineament data and limited distribution of joint data. The comparison of lineament data from the Boret area to joint data from sites 1, 2 and 4 illustrates this point. The two dominant joint sets, a major E-NE spread of joints and a minor but well-defined NW trend, are much better defined than the range of lineaments in generally NE and NW orientations. In the area around site 3 at Stempelen, where joint data is also available to compare with lineament orientations, the two joint sets strike NE and NNW, while the lineaments show a major N-S trend. However, this discrepancy between the data sets may be due to the scarcity of the lineament data from this area. In the other subareas where no joint data is available for comparison, the lineaments have a major NE-NNE trend which has a wide spread of orientations. Two of the four subareas also show a minor NW trend of lineaments.

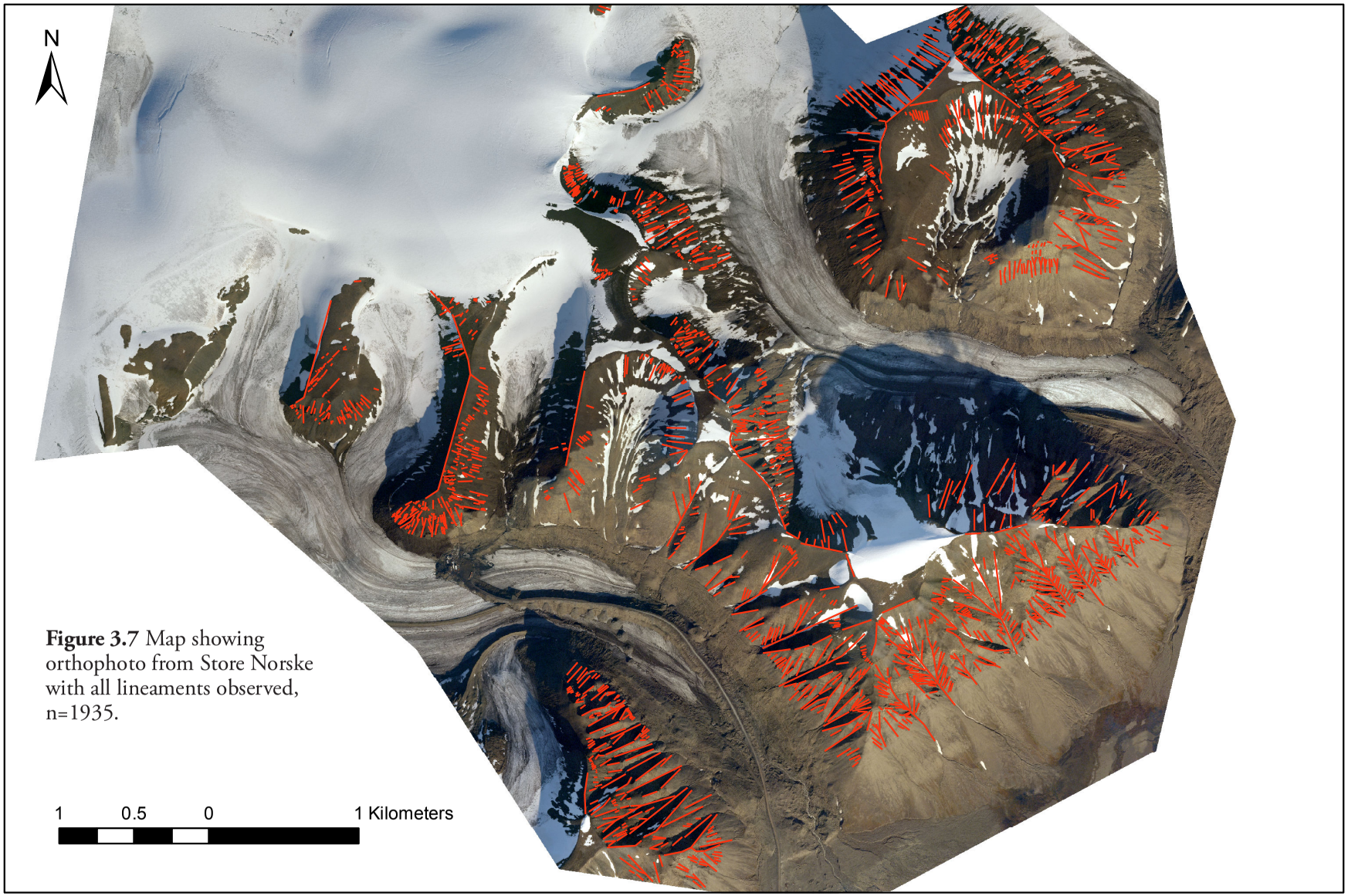

Figure 3.7 Map showing orthophoto from Store Norske with all lineaments observed, n=1935.

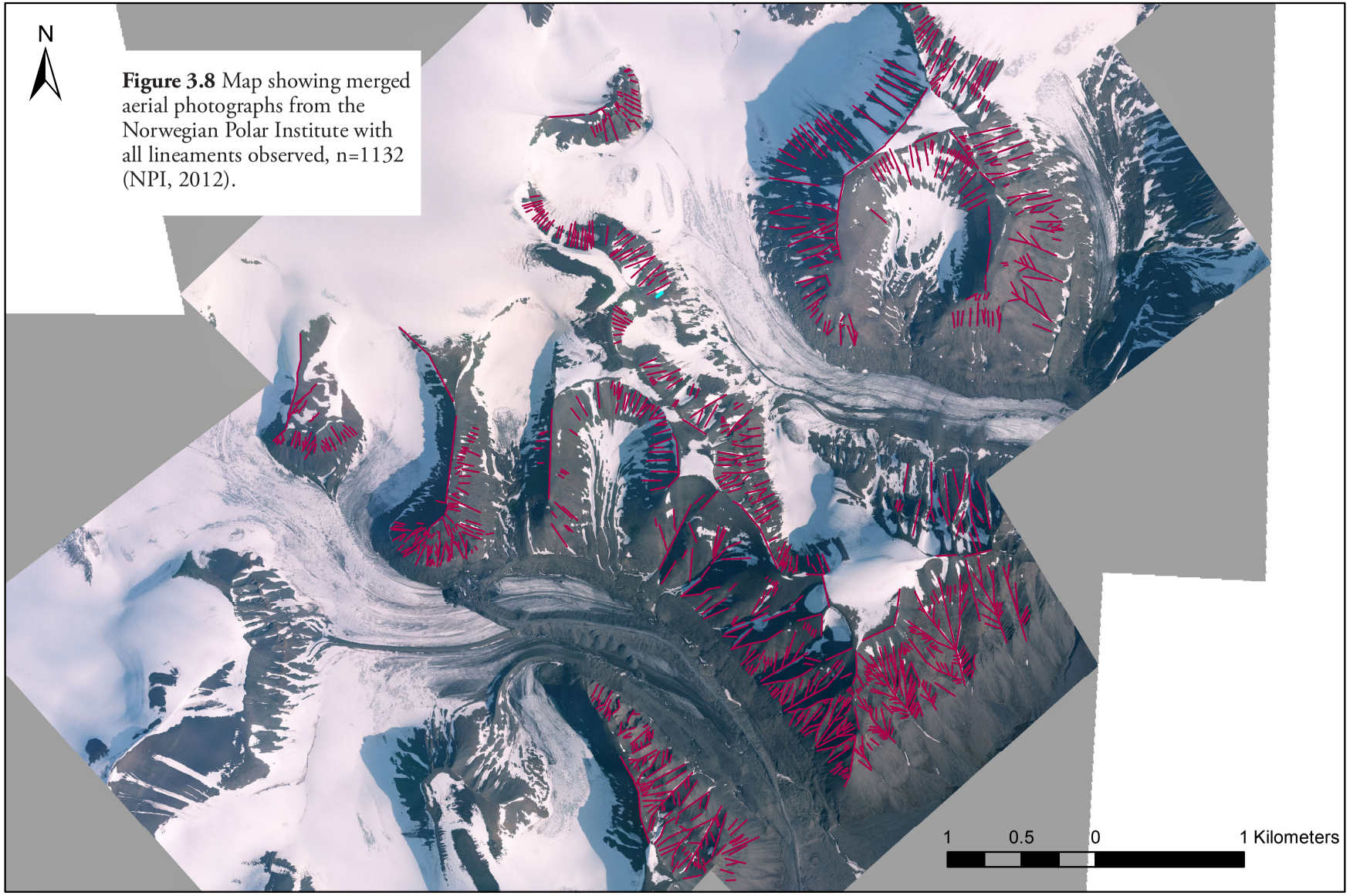

Figure 3.8 Map showing merged aerial photographs from the Norwegian Polar Institute with all lineaments observed, n=1132 (NPI, 2012).

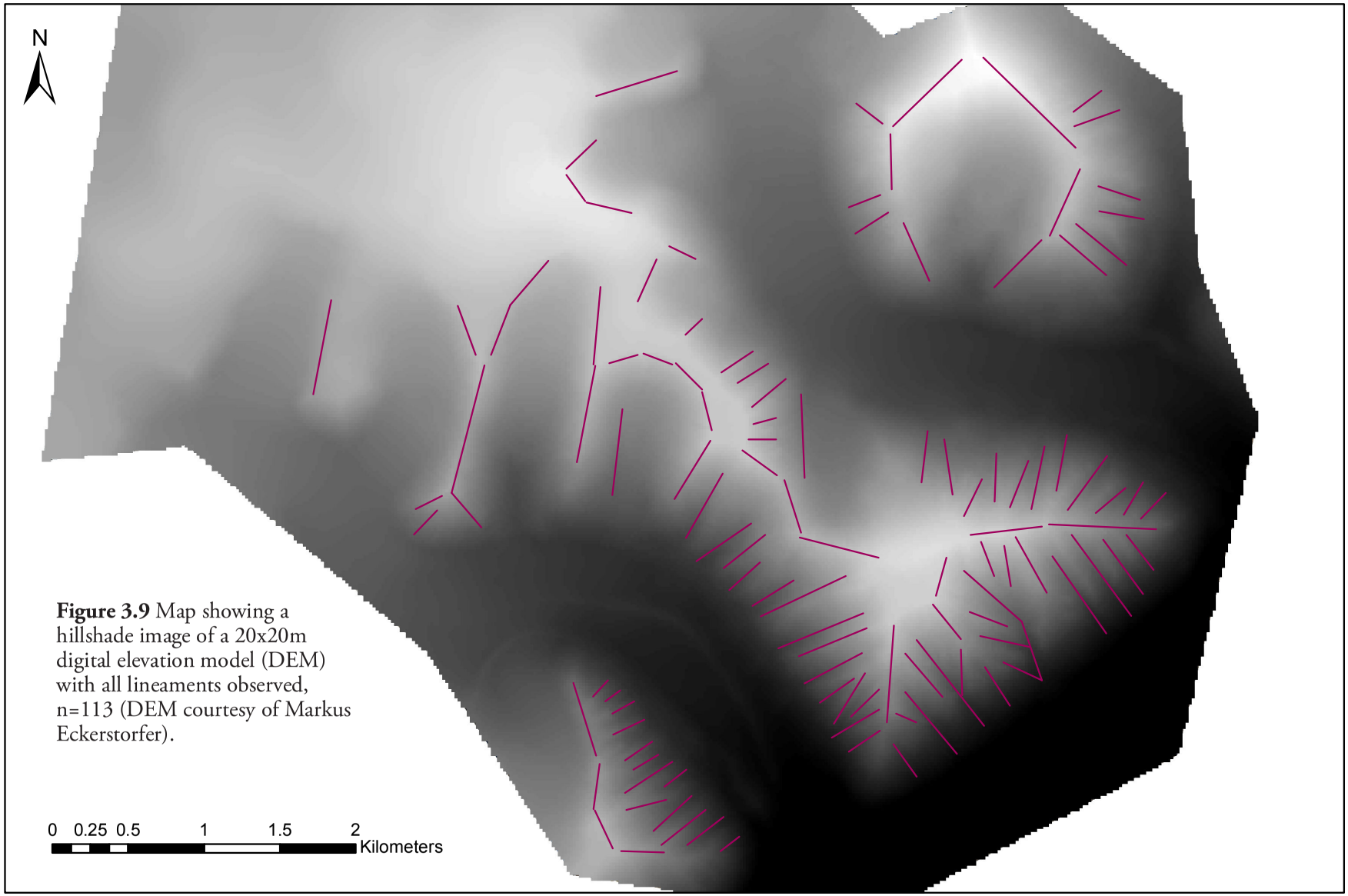

Figure 3.9 Map showing a hillshade image of a 20x20m digital elevation model (DEM) with all lineaments observed, n=113 (DEM courtesy of Markus Eckerstorfer).

Discussion

Overview

The analyses of brittle structures in the Svea region yield paleostress orientations for each type of structure: normal and thrust faults, joints, and lineaments. As the faults are the most reliable paleostress indicators and smaller structures are most likely related to them, this discussion will compare the joint and lineament-resolved paleostress orientations to the fault-resolved paleostress orientations to see whether the findings support each other. Based on their resolved paleostress regimes, these structures will then be related to documented structures of previous studies and existing theories/models of Paleogene tectonic processes. Though the thrust faults can be easily correlated with other major thrusts resulting from the main stresses of fold-and-thrust belt formation, the origins of the normal faults are more difficult to constrain. Three possible tectonic setting are proposed for the origins of the normal faults: 1) extension in response to the over-thickened fold-and-thrust belt wedge, 2) post-orogenic extension during the transtensional rifting of Svalbard and Greenland, or 3) the general transpressive setting of the fold-and-thrust belt. The third hypothesis is the simplest, suggesting that both the thrust and normal faults formed in the same transpressive stress regime during the main stages of the fold-and-thrust belt evolution.

Paleostress Interpretations

Normal and thrust fault stress regimes

The normal faults observed at the surface which correlate with faults observed in the mine (faults 1-4) cut the Firkanten through Grumentbyen Formations (visible in the mountainside above the mine entrance, Figure 3.4a). This indicates that they are younger than the age of the Grumantbyen Formation, which is Late Paleocene (Dallmann, 1999). The thrust faults are only observed in the mine within the Firkanten Formation, which implies that they are younger than Early Paleocene.

In general, the fault map (Figure 3.5) shows two distinct orientations of faults: NNW-SSE striking, west-dipping thrust faults and ENE-WSW striking, NNW or SSE dipping normal faults. As no fault slip analysis of the thrust faults was done, a basic paleostress reconstruction based on the premise that fault slip was perpendicular to fault strike shows ENE directed compression.

More thorough investigation of the normal faults in the study area shows multiple small-scale associated faults that can be related to the same fault system and

deformational event. Based on their orientations and location in the mine, faults 5, 6, 7, and 8 can be related to a single fault system. The variability in the number of fault segments in a given location, and the fact that the individual fault segments show variable displacement, indicates a branching fault system with segments that likely taper out. The orientation of this fault system suggests that it continues across the next panel that is currently slated to be mined, though given the variability in fault strike along the mapped portions, its exact position cannot be determined.

In contrast to the normal faults mapped in the mine, the fault at site 3 is a low angle normal fault with a dip of 32°. Its NNW-SSE orientation is nearly perpendicular to the strikes of the mine faults. However, as it was not possible to determine the fault's displacement from the field data and because the fault was only observed for a few meters along the outcrop face, this fault is assumed to be relatively small. As slickenlines on the fault plane showed a down-dip slip direction, it was included in the fault slip analysis.

The fault slip analysis of normal fault segments mapped in the mine and the site 3 fault gives σ_1 oriented sub-horizontally NNW, σ_2 oriented sub-vertically and σ_3 oriented horizontally ESE (Figure 3.6). These results indicate NNE-SSW extension, which is perpendicular to the ENE-directed compression proposed for the thrust faults. However, given the transpressive setting during most of the Paleogene, it is possible that both fault systems formed in the same transpressional stress regime. The faults are by far the most reliable paleostress indicators, as they are the largest structures and show the greatest deformation. But since fractures are often associated with faults, it is reasonable to expect the joint and lineament analyses to yield similar paleostress orientations.

Joint-derived stress regimes

Joints, like faults, must be younger than the rocks they cut and so in the study area, the ages of the joints can be constrained based on the ages of the sandstone units that they are observed in. Given that joints were observed in the Firkanten (Early Paleocene) and Grumantbyen (Late Paleocene) Formations (Dallmann, 1999), they must have formed after the Early Paleocene and Late Paleocene respectively. However, since two sets of similarly oriented joints are seen in both the Firkanten and Grumantbyen Formations, it is reasonable to assume that they are the product of the same stress regime and formed at the same time, and therefore are younger then Late Paleocene.

Conjugate joint model

The two dominant joint sets observed in each of the four mapping sites and the lack

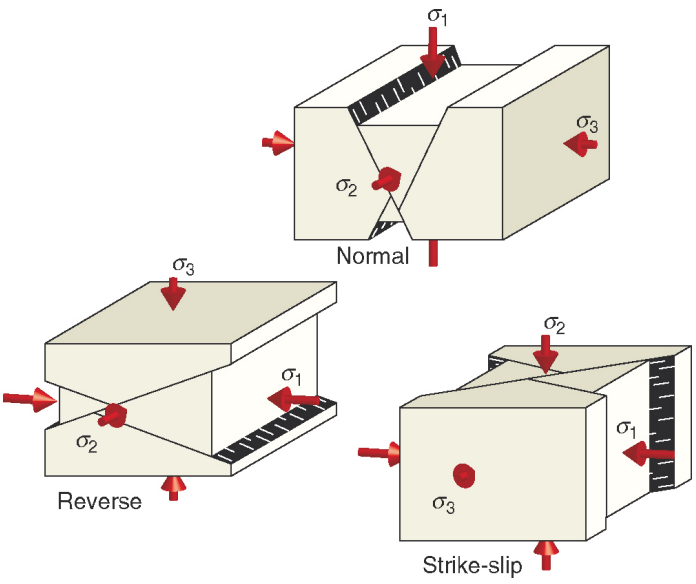

Figure 4.1 Block diagrams showing pairs of conjugate faults and their correpsonding orientations of principal stress, σ_1, σ_2, and σ_3. Similar stress regimes can be resolved for pairs of conjugate fractures. Note that in a strike-slip setting, σ_2 is oriented vertically while σ_1 and σ_3 are oriented horizontally. From Fossen, 2010, Figure 9.5.

of observed cross-cutting relationships at sites 1-3 lead to the assumption that these two groups formed as a conjugate joint set. Paleostress analysis of these conjugate joint sets at each site shows σ_1 and σ_3 oriented horizontally, while σ_2 is oriented vertically, a stress regime typical of a strike-slip tectonic setting (Figure 4.1; Fossen, 2010). However, the σ_1 and σ_3 directions resolved at sites 1 and 3 conflict with those resolved at sites 2 and 4. This might suggest the possibility of two discrete stress regimes. But the similarity in the trends of the average joint sets at all sites support the initial assumption that all conjugate joints formed under a single stress regime. The varying orientations of σ_1 could be due to variability in the joint measurements or the scarcity of data at sites 2-4. As the two joint sets are nearly perpendicular, a slight change in the orientation of one of the joint sets is enough to change the acute angle, and therefore σ_1, by 90°. Therefore, as the majority of the joint measurements were taken at site 1, it seems reasonable to apply this reconstructed paleostress regime of NW-SE compression and NNE-SSW extension to the study area as a whole.

However, when comparing the paleostress regime resolved from the fault data to that of the joint data, some discrepancies appear that call into question the initial conjugate joint assumption. The conjugate joints' stress regime of NW-SE compression and NNE-SSW extension does not correlate well with the faults' stress regime of ENE-WSW compression and NNE-SSW extension. The acute angles between the two joint sets are also larger than is typical for conjugate joints. At all four sites, the acute angle between the joint sets is greater than 70°, while according to Dunne and Hancock (1994), the maximum acute angle for conjugate shear fractures is 60°.

Extensional, two-phase joint model

Consequently, it is possible that the initial conjugate joint assumption is incorrect, and that these joint sets in fact formed as mode I extensional joints in two phases of deformation. The orientations of both joint sets correlate well with the orientations of the thrust and normal faults. The more dominant joint set (ENE-WSE) has a similar orientation to the normal faults, approximately perpendicular to the strike of the thrust faults. The less numerous joint set (NNW-SSE) has a similar orientation to the thrust faults. Though this fact in itself does not indicate that both types of structures formed under similar stress regimes, a similar relationship between joints and larger compressional structures has been observed in the foreland of the Appalachian mountain belt (Diamond et al., 1975; Engelder and Geiser, 1979; Engelder, 1985; Engelder 1993).

A number of studies have focused on mapping joints in the Appalachian plateau region of western Pennsylvania and New York. Mapping reveals a dominant systematic joint set which trends perpendicularly to the Appalachian mountain belt and the major folds (Diamond et al., 1975; Engelder and Geiser, 1979; Engelder, 1985; Engelder 1993). Engelder (1985) interprets these joints as mode I tectonically-derived fractures which formed in response to the stresses of the Alleghenian Orogeny (with σ_3 parallel to the trend of the orogenic belt). A second, less dominant joint set, which trends parallel to the fold belt, truncates at the first joint set. Engelder (1985) interprets these joints as younger, post-orogenic, release joints that formed in response to removal of the overburden sediments during uplift and erosion. In the coal mines of western Pennsylvania, these two joint sets influence the layout of the mines since coal breaks along these planes. Mine tunnels are driven parallel to these systematic joints, with the major transport tunnels generally following the dominant joint set (Davis, 2011).

The two joint sets in the Svea region are strikingly similar to the joints in the Appalachian foreland. The more numerous joint set strikes ENE-WSW, perpendicular to the trend of the thrust faults in the area and the larger structures of the fold-and-thrust belt. The few cross-cutting relationships observed at site 4 indicate that this joint set formed first. This evidence points to a tectonic origin for this dominant joint set as a result of fold-and-thrust belt stresses.

The less numerous joint set in the study area strikes NNW-SSE, perpendicular to the dominant joint set and parallel to the trend of the fold-and-thrust belt. This orientation and the cross-cutting relationships at site 4 suggest that, like the second joint set in the Appalachian plateau, they are release joints formed during erosion of the overburdening material. This is plausible, as since the Paleogene, uplift of Svabard has removed at least 2000m of strata (Orheim, 1982). Release joints form when

planes which have been normal to the greatest compressive stress release, and so are influenced by tectonic stresses though not actually caused by them. This means that in a fold-and-thrust belt setting release joints form parallel to the major fold and thrust axes but post-date the main stages of deformation (Engelder, 1985). The field data from the Svea region fit well with this interpretation.

Lineament-derived stress regimes

The lineament data show a major NE-SW to NNE-SSW trend, and a minor NW-SE trend. If the lineaments are assumed to form along weak bedrock planes, rather than as purely topographically-controlled features, then their orientations should be able to give some indication of paleostress. In this case, the lineaments were assumed to have formed along pre-existing fracture systems. Working with this assumption, the main lineament trends indicate NW-SE extension and ENE-WSW extension. However, there are some major assumptions involved with the lineament analysis that should be addressed.

The first of these assumptions is that the linear erosional features observed in the aerial images of the study area are in fact related to bedrock fractures. However, bedrock outcrops in the Svea region are confined to the more resistant cliff-forming sandstone units, and a great deal of the landscape surface is covered with erosional talus and scree, particularly from the more easily eroded shale units. Most of the lineaments observed in the aerial images run perpendicular to the slopes, and it is difficult to know to what extent they are caused by bedrock weaknesses or simply by local topography. There are two general lineament trends, but it is possible that the majority of lineaments are oriented this way because the main valleys in the study area run NW-SE and most lineaments are erosional features which run straight downslope, perpendicular to the trend of the valleys. Though it is quite possible that pre-existing bedrock weaknesses influenced the orientation of the main glacial valleys in the region, the local topography is not sufficient evidence for paleostress orientations. A lineament analysis such as this would yield much more conclusive results in an area with continuously well-exposed bedrock and not much variation in local topography.

Tectonic Origins of Brittle Deformation

Though no previous studies have focused on small-scale structures in the Svea region, work has been done on the large fold-and-thrust belt system in western Spitsbergen and also on the large anticlines to the east of the study area that represent the southern termini of the Billefjorden and Lomfjorden fault zones (Haremo and Andresen, 1992; Bergh et al., 1997; Braathen et al., 1999). The literature relates

these structures to the proposed 5-stage kinematic model for the evolution of the West Spitsbergen fold-and-thrust belt (Kleinspehn et al., 1989; Braathen and Bergh, 1995). The kinematics of the different stages vary in the different structural provinces of Svalbard, and as a result correlating the small-scale structures in the foreland with larger structural features of the western region is difficult. Nonetheless, it is possible to obtain a general understanding of the tectonic origins of the Svea structures by relating them to larger structural features of the similar orientations with well-constrained paleostress regimes. As the joints and lineaments are most likely related to the faults, the faults will be the focus of the following discussion on the possible origins of Paleogene deformation in the Svea region.

Origins of thrust faults

The thrust faults in the mine can be well correlated with fault data presented by Braathen et al. (1999) from the foreland in Lomfjorden, as they are similarly oriented and show the same vergence, indicating ENE-directed compression (Figure 4.2). Braathen et al. (1999) relate these structures to stages 2 and 3 of the 5-stage kinematic model for the fold-and-thrust belt, which encompassed the majority of crustal wedge thickening. As the thrust faults are located in the Firkanten Formation, which is Early Paleocene, and stages 2 and 3 of the fold-thrust belt evolution occurred from the Late Paleocene to Late Eocene, the ages of the faults can be constrained as Early Paleocene – Late Eocene.

Origins of normal faults

The origins of the normal faults in the Svea region are not so apparent, as larger-scale faults of similar orientations are not documented in the literature, either in the western fold-and-thrust complex or the foreland basin. These normal faults may have formed in one of three possible tectonic systems: 1) extension in response to the over-thickened fold-and-thrust belt wedge, 2) the post-orogenic transensional rifting of Svalbard and Greenland, or 3) the transpressive stress regime that formed the thrust faults during the main stages of the fold-and-thrust belt evolution. The structural evidence which supports and contests each mechanism for the origins of the normal faults is discussed below.

Collapse of the fold-and-thrust belt wedge

The proposed critical wedge model for the West Spitsbergen fold-and-thrust belt chronicles the evolution of the wedge from a critical taper geometry (stage 2), to a supercritical taper (stages 3-4) by imbrication and underplating, and adjustment back to a critical taper (stage 4-5) by normal faulting and erosion (Figure 4.2; Braathen et al., 1999; Platt, 1986). At first glance, it appears that the normal faults in the Svea region may well have formed in response to this overthickened fold-and-thrust

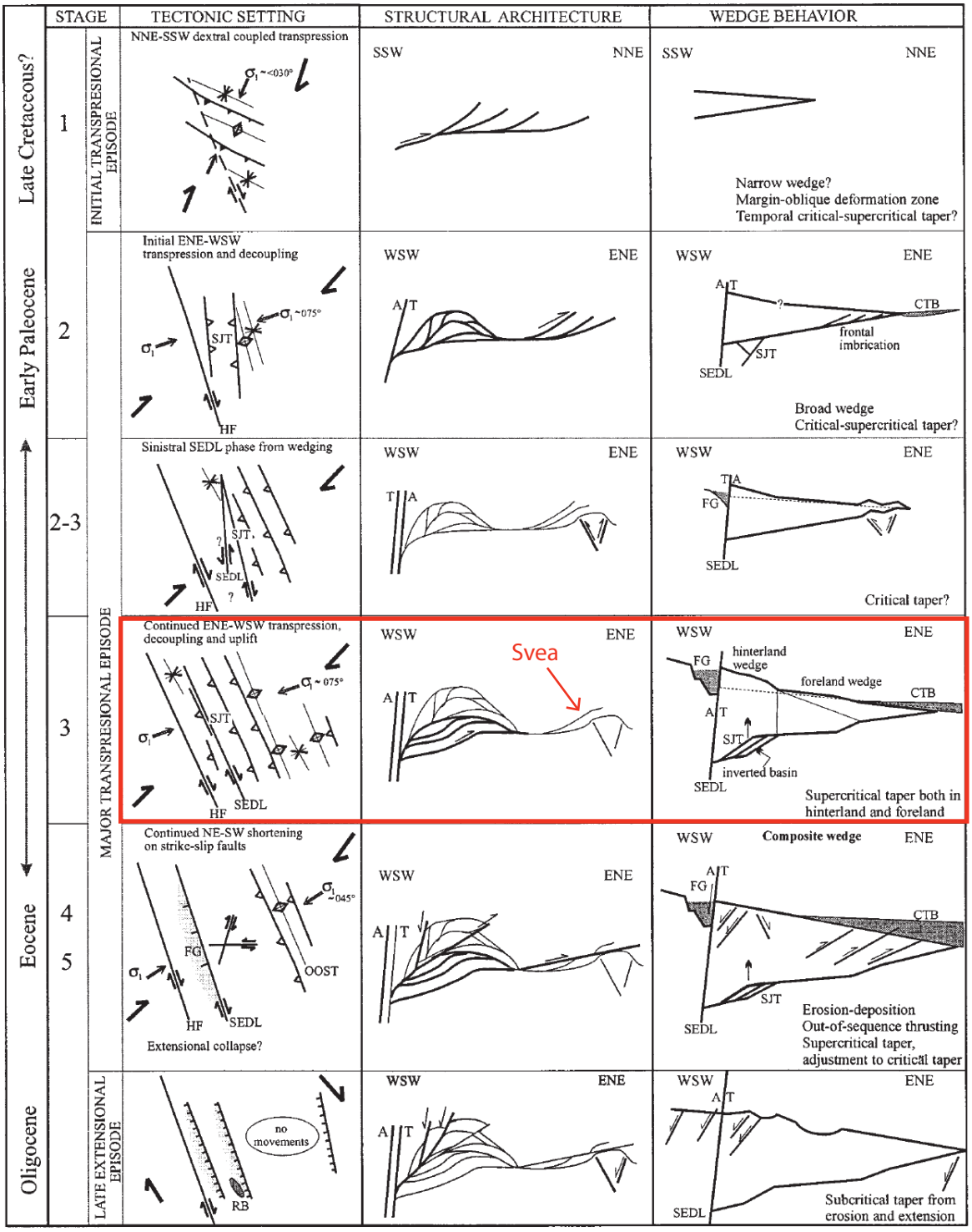

Figure 4.2 Summary of the tectonic evolution of the West Spitsbergen fold-and-thrust belt according to Braathen et al. (1999), showing the age, tectonic setting, stress regime, key structures, schematic cross-section and critical wedge model for each of the 5 stages of deformation. Stage 3 of deformation is highlighted as it best corresponds to the brittle deformation in the Svea region. Thick half-arrows show the relative motion between the Greenland and Svalbard plates. CTB stands for the Central Tertiary Basin. Other abbreviations are structures not discussed in this text (modified from Braathen et al., 1999; Fig. 10).

belt wedge. However, a closer look at both the orientations of faults analyzed by Braathen et al. (1999) and their locations suggest otherwise. In stage 4 of Braathen et al.'s (1999) kinematic model, coupled dextral transpresssion results in conjugate transcurrent faults oriented with their acute angle bisector at 45° and normal faults also striking 45°, indicating NW-SE extension. Though this paleostress regime is similar to the NNW-SSE extension implied by the normal faults in the Svea region, the NE striking normal faults observed by Braathen et al. (1999) are located in the western basement-involved domain of the fold-and-thrust belt, and no such structures are seen in the foreland province. This agrees with Platt's (1986) model of a critical wedge, where extensional collapse occurs behind the thrust front and not in the foreland province. This implies that the normal faults in the Svea region are probably not linked to wedge collapse.

Post-orogenic rifting

According to the kinematic model for the fold-and-thrust belt, the adjustment to a critical wedge taper geometry (stage 4) was followed by post-orogenic extension (stage 5; Kleinspehn et al., 1989; Braathen and Bergh, 1995; Bergh et al., 1997; Braathen et al., 1999). This extensional episode might be a possible mechanism for the normal faulting in the Svea region, were it not for the incompatibility of the field data with previously documented structures. During stage 5, deformation was localized along N-S trending faults in the hinterland (now offshore of western Spitsbergen) and in the eastern foreland, along the Billefjorden and Lomfjorden fault zones (Figure 4.2; Braathen et al., 1999; Leever et al., 2011). Normal fault orientations in the Svea region do not fit well with this accepted post-orogenic E-W extensional regime of the Late Eocene – Oligocene (Figure 4.2, Braathen et al., 1999).

Syntectonic transpression

The normal faults in the Svea region cannot be well correlated with a specific stage of fold-and-thrust belt formation because there are no previously documented examples of ENE-trending normal faults showing NNW-SSE extension in the western provinces of the fold-and-thrust belt. This study is limited to comparing the paleostress regime of the normal faults with the resolved paleostress regimes of previous studies. Based on their stress regime of σ_3 oriented NNW-SSE and σ_1 oriented ENE-WSW, the normal faults fit best with stages 2 and 3 of the fold-and-thrust belt formation which involved ENE-directed transport. A theoretical strain ellipse for Spitsbergen's transpressive setting during the Paleocene-Eocene, based on Harding's (1973; 1974) simple shear model, shows the various structures expected to form in a dextral transpressive setting (Figure 4.3c). Compressional structures such as thrust faults and folds are expected to form with strikes parallel to the maximum strain axis, or direction of maximum extension, of the strain ellipse. Normal faults are

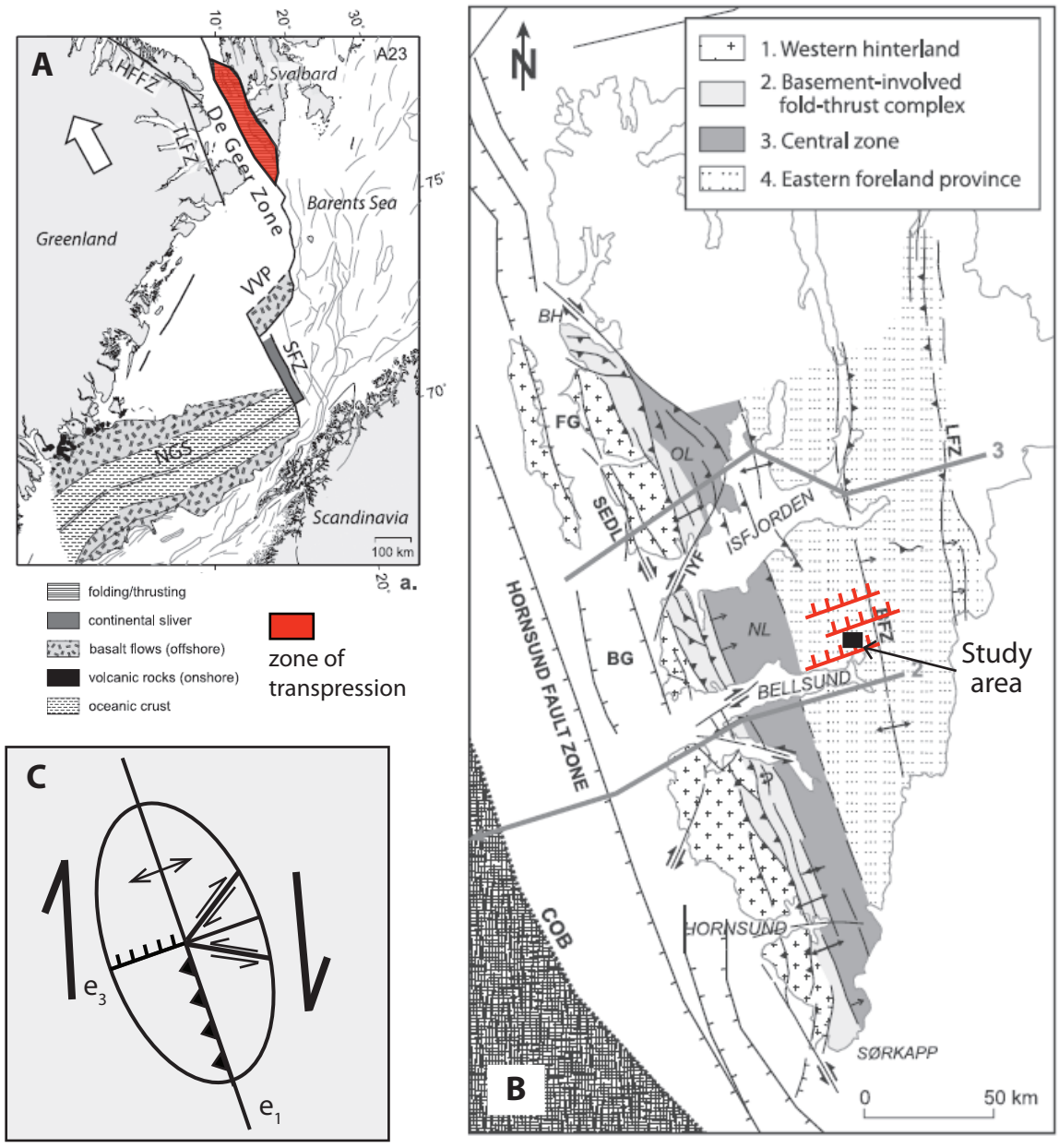

Figure 4.3 a) Tectonic plate reconstruction from the Paleocene showing the location of Svalbard, Greenland, the Hornsund/De Geer Fracture Zone and the resulting fold-and-thrust belt (modified from Leever et al., 2011). b) Structural map of Spitsbergen, showing the main provinces of the West Spitsbergen fold-and-thrust belt, major fault zones and folds and the approximate orientation of the normal faults observed in the Svea region (note the exaggerated scale) (modified from Leever et al., 2011). c) Harding's (1973; 1974) theoretical strain ellipse with typical structures seen in a dextral transpressive setting, modified from Krantz (1995). The maximum strain axis, or direction of maximum extension, is indicated by e_1, while the minimum strain axis is indicated by e_3.

expected to form with strikes oriented parallel to the short axis of the strain ellipse, perpendicular to the maximum strain axis. Given the orientation of the normal faults in the model strain ellipse, the origins of the normal faults in the Svea region can be tentatively constrained as a result of the general transpressive setting of the Paleocene-Eocene. This suggests that they formed concurrently with the thrust faults, although this relationship cannot be resolved without the observation of cross-cutting relationships. In conclusion, the data suggest that the brittle deformation in the Svea region is the result of the overall transpressional tectonic system during the Paleocene-Eocene.

Conclusion

Currently, there is no consensus on the origins of the brittle deformation in the Svea region, as the small-scale faults and fractures have not been studied in detail. This study not only located and predicted faults in the Svea Nord mine, but also attempted to relate the brittle deformation to the tectonic evolution of the West Spitsbergen fold-and-thrust belt. Results show two series of faults: and ENE-WSW striking set of normal faults which indicate NNW-SSE extension, and a NNW-SSE striking, W-dipping set of thrust faults which indicate ENE-directed compression. Two orientations of subvertical joints were observed in the field, which correspond to the orientations of the faults. The ENE-striking joint set is both more numerous and more variable than the NNW-striking joint set. Two general lineament systems, a numerous NE trend and minor NW trend, were resolved from aerial images.

When relating the structures in the Svea region with well documented structures in the western, basement-involved province of the fold-and-thrust belt, it appears that there are three possible interpretations as to the tectonic origins of these extensional brittle structures: 1) extension in response to the overthickened fold-and-thrust belt wedge, 2) post-orogenic extension due to the rifting of Svalbard and Greenland, and 3) the general transpressive setting during the main stages of fold-and-thrust belt formation. The first two possibilities can be discounted as mechanisms for normal fault formation, as the orientations and reconstructed paleostress regimes of the Svea faults do not fit well with those of previously documented structures from these stages. The third model of a transpressive system is the most plausible, as the theoretical strain ellipse for this setting shows normal faults forming parallel to σ_1, with an ENE-WSW orientation, similar to the faults observed in the Svea region.

Future work

Although the results of this study reveal the general tectonic history of the Svea region during the Paleogene, some questions still need to be answered to better understand the various phases of deformation in the Svea region at this time. Constraining the relationships between the thrust faults and the normal faults and the relationships between the two joint sets is crucial to resolving the region's deformational history. A detailed survey of possible locations within the mine where cross-cutting relationships might be observed would be beneficial. More comprehensive mapping of fractures in surficial outcrops will yield more concrete evidence of relative joint set ages and resolve the question as to whether the joints are conjugate or not. Locating more faults exposed at the surface to the east of the Svea Nord mine would also be helpful. If all the thrust faults and normal faults were identified in the study area, local

shortening and extension could be quantified. It would also be important to look at some brittle structures to the east of Svea around the Billefjorden and Lomfjorden fault zones. Because there is evidence that these faults were re-activated during the Paleogene, their movements likely influenced the small-scale structures around Svea. Comparing brittle structures proximal to the fault zones with the structures in Svea would reveal to what degree movements along these faults zones caused deformation in Svea.

References

Allmendinger, R.W., 2012a, FaultKin: Http://www.Geo.Cornell.edu/geology/faculty/RWA/programs/, v. 5.

Allmendinger, R.W., 2012b, Stereonet: Http://www.Geo.Cornell.edu/geology/faculty/RWA/programs/, v. 8.

Andresen, A., Haremo, P., Swensson, E., and Bergh, S. G., 1992, Structural geology around the southern termination of the Lomfjorden fault complex: Agardhdalen, East Spitsbergen: Norsk Geologisk Tidsskrift, v. 72, p. 83-91.

Angelier, J., 1994, Fault Slip Analysis and Palaeostress Reconstruction, in Hancock, P.L., ed., Continental Deformation: Oxford, England, Pergamon Press, p. 53-100.

Bergh, S. G., Braathen, A., and Andresen, A., 1997, Interaction of Basement-Involved and Thin-Skinned Tectonism in the Tertiary Fold-Thrust Belt of Central Spitsbergen, Svalbard: The American Association of Petroleum Geologists, v. 81, p. 637-661.

Bergh, S. G., Maher Jr., H. D., and Braathen, A., 2000, Tertiary divergent thrust directions from partitioned transpression, Brøggerhalvøya, Spitsbergen: Norsk Geologisk Tidsskrift, v. 80, p. 63-82.

Bons, P. D., Elburg, M. A., and Gomez-Rivas, E., 2012, A review of the formation of tectonic veins and their microstructures: Journal of Structural Geology, v. 43, p. 33-62.

Braathen, A., and Bergh, S. G., 1995, Kinematics of Tertiary deformation in the basement-involved fold-thrust complex, western Nordenskiøld Land, Svalbard: tectonic implications based on fault-slip data analysis: Tectonophysics, v. 249, p. 1-29.

Braathen, A., Bergh, S. G., and Maher Jr., H. D., 1999, Application of a critical wedge taper model to the Tertiary transpressional fold-thrust belt on Spitsbergen, Svalbard: Geological Society of America Bulletin, v. 111, .

Braathen, A., Bergh, S. G., and Maher Jr., H. D., 1997, Thrust kinematics in the central part of the Tertiary transpressional fold-thrust belt in Spitsbergen: Norges Geologiske Undersøkelse Bulletin, v. 433, p. 32-33.

Braathen, A., Bergh, S. G., and Maher Jr., H. D., 1995, Structural outline of a Tertiary Basement-cored uplift/inversion structure in western Spitsbergen, Svalbard: Kinematics and controlling factors: Tectonics, v. 14, p. 95-119.

Braathen, A., Braathen, A., Bergh, S. G., Dallmann, W., and Harland, W. B., 1995, Tertiary or Cretaceous age for Spitsbergen's fold-thrust belt on the Barents Shelf: Tectonics, v. 14, p. 1321-1326.

Castro, C., 2010, Paleostress analysis of Mesozoic fractures and basalt dikes in Tuckerman Ravine, New Hampshire: Bates College Department of Geology, p. 1-60.

Dallmann, W. K., 1999, Lithostratigraphic Lexicon of Svalbard: Oslo, Norsk Polarinstitutt, p. 318.

Dallmann, W. K., 1993, Tertiary fold-and-thrust belt of Spitsbergen, Svalbard: Norsk Polarinstitutt, , 1-46 p.

Dallmann, W. K., Ohta, Y., and Andresen, A., 1988, Tertiary Tectonics of Svalbard: Extended abstracts from Symposium held in Oslo 26 and 27 April 1988: Norsk Polarinstitutt, Report 46.

Davis, G. H., Reynolds, S. J., and Kluth, C. F., 2012, Structural Geology of Rocks and Regions, 3rd edition: New Jersey, USA, John Wiley & Sons, Inc., p. 839.

Dunne, W.M., and Hancock, P. L., 1994, Palaeostress Analysis of Small-Scale Brittle Structures, in Hancock, P. L., ed., Continental Deformation: Oxford, England, Pergamon Press, p. 101-120.

Haremo, P., and Andresen, A., 1992, Tertiary decollement thrusting and inversion structures along Billefjorden and Lomfjorden Fault Zones, East Central Spitsbergen, in Larsen, R.M., Brekke, H., Larsen, B.T. and Talleraas, E., eds., Structural and Tectonic Modelling and its Application to Petroleum Geology: Amsterdam, Norwegian Petroleum Society, p. 481-494.

Ingólfsson, Ó., 2011, Fingerprints of Quaternary glaciations on Svalbard: Geological Society Special Publication, v. 354, p. 15-31, doi: 10.1144/SP354.2.

M. Jakobsson, L. A. Mayer, B. Coakley, J. A. Dowdeswell, S. Forbes, B. Fridman, H. Hodnesdal, R. Noormets, R. Pederson, M. Rebesco, H.-. Schenke, Y. Zarayskaya, A. D. Accettella, A. Armstrong, R. M. Anderson, P. Bienhoff and A. Camerlenghi. , 2012, The International Bathymetric Chart of the Arctic Ocean (IBCAO), Version 3.0: Geophysical Research Letters, .

Jochmann, M., 7/2012, Fieldwork planning session: personal communication.

Jochmann, M., 2/29/12, Coal on Svalbard lecture: personal communication.

Kindley, C., 2011, Paleostress analysis of Mesozoic extension in fractures and basalt dikes, Great Gulf, NH: Bates College Department of Geology, p. 1-92.

Krantz, R.W., 1995, The transpressional strain model applied to strike-slip, oblique-convergent and oblique-divergent deformation: Journal of Structural Geology, v. 17, p. 1125-1137.

Leever, K. A., Gabrielsen, R. H., Faleide, J. I., and Braathen, A., 2011, A transpressional origin for the West Spitsbergen fold-and-thrust belt: Insight from analog modeling: Tectonics, v. 30, , doi: 10.1029/2010TC002753.

Mabee, S. B., Hardcastle, K. C., and Wise, D. U., 1994, Method of collecting and analyzing lineaments for regional-scale fractured-bedrock aquifer studies: Ground Water, v. 32, p. 884-894.

Maher Jr., H.D., Craddock, C., and Maher, K., 1986, Kinematics of Tertiary structures in upper Paleozoic and Mesozoic strata on Midterhuken, west Spitsbergen: Geological Society of America Bulletin, v. 97, p. 1411-1421.

McCann, A.J., and Dallmann, W.K., 1996, Reactivation history of the long-lived Billefjorden Fault Zone in north central Spitsbergen, Svalbard: Geological Magazine, v. 133, p. 63-84.

Norwegian Polar Institute, N., 2012, TopoSvalbard: (http://toposvalbard.npolar.no10/25 2012).

Orheim, A., 1982, Undiscovered coal resources of Svalbard: An assessment using Monte Carlo Simulation: Arctic Geology and Geophysics: Proceedings of the Third International Symposium on Arctic Geology, Memoir 8, 339-413.

Salvigsen, O., Winsnes, T. S. and Steel. R., 1989, Braganzavågen C10G: Geologic Map Svalbard, scale 1:100,000, 1 sheet(s).

Store Norske Spitsbergen Kulkompani, AS, 2012, Store Norske: mining in the high north: (www.snsk.no10/25 2012).

Worsley, D., 2008, The Post-Caledonian development of Svalbard and the western Barents Sea: Polar Research, v. 27, p. 298-317, doi: 10.1111/j.1751-8369.2008.00085.x.

Worsley, D., 1986, The Geological History of Svalbard: Stavangar, Den Norske Stats Oljeselskap A.S., p. 121.